Characterization of Underground Facilities

Study Leader:
W. Happer
[redacted]

Contributors:
J. Cornwall
A. Despain
D. Eardley
R. Garwin
D. Hammer
R. Jeanloz
J. Katz
O. Rothaus
M. Ruderman
R. Schwitters
S. Treiman
J. Vesecky

April 1999

JSR-97-155

JASON
The MITRE Corporation
1820 Dolley Madison Boulevard
McLean, Virginia 22102-3481
(703) 883-6997

REPORT DOCUMENTATION PAGE

Form Approved
OMB No. 0704-0188

1. AGENCY USE ONLY (Leave blank)	2. REPORT DATE	3. REPORT TYPE AND DATES COVERED
	April 12, 1999	

4. TITLE AND SUBTITLE

Characterization of Underground Facilities

5. FUNDING NUMBERS

13-988534-A4

6. AUTHOR(S)

H. Abarbanel, J. Cornwall, A. Despain, D. Eardley, R. Garwin, D. Hammer, R. Jeanloz, J. Katz, O. Rothaus, M. Ruderman, R. Schwitters, S. Treiman , J. Vesecky

7. PERFORMING ORGANIZATION NAME(S) AND ADDRESS(ES)

The MITRE Corporation
JASON Program Office
1820 Dolley Madison Blvd
McLean, Virginia 22102

8. PERFORMING ORGANIZATION REPORT NUMBER

JSR-97-155

9. SPONSORING/MONITORING AGENCY NAME(S) AND ADDRESS(ES)

Defense Advanced Research Projects Agency
3701 North Fairfax Drive
Arlington, Va. 22203-1714

10. SPONSORING/MONITORING AGENCY REPORT NUMBER

JSR-97-155

11. SUPPLEMENTARY NOTES

12a. DISTRIBUTION/AVAILABILITY STATEMENT

Approved for public release, distribution unlimited.

Review of this material does not imply Department of Defense indorsement of factual accuracy or opinion.

12b. DISTRIBUTION CODE

Distribution Statement A

13. ABSTRACT *(Maximum 200 words)*

JASON undertook a study at DARPA's request to look for new opportunities for progress in the detection and characterization of UGFs. Part of our charge was to identify the most promising technology areas for investment, emphasizing standoff and covert sensor techniques. The study therefore surveyed a wide range of approaches, and we received numerous briefings. These included summaries of the technology programs of various agencies and briefings from organizations and companies on specific technology approaches. In addition various new ideas were suggested by JASON contributors.

14. SUBJECT TERMS

15. NUMBER OF PAGES

16. PRICE CODE

17. SECURITY CLASSIFICATION OF REPORT	18. SECURITY CLASSIFICATION OF THIS PAGE	19. SECURITY CLASSIFICATION OF ABSTRACT	20. LIMITATION OF ABSTRACT
Unclassified	Unclassified	Unclassified	SAR

Contents

1 INTRODUCTION

Detection and characterization of underground facilities (UGFs) is a difficult but important problem. Underground facilities are being used to conceal and protect critical activities that pose a threat to the United States. These include the development and storage of weapons of mass destruction, principally nuclear, chemical, and biological weapons. Underground facilities can also protect critical C^3 installations and national leadership.

Hundreds of underground installations have been constructed worldwide and many more are under construction. The proliferation of such facilities is a legacy from the Gulf War: a lesson from this war was that almost any above-ground facility is vulnerable to attack and destruction by precision guided weapons. To counter this vulnerability, many countries have moved their assets underground.

Underground facilities not only protect critical activites but also conceal them. Once built, it may be very difficult to determine the nature of the facility. Conventional methods, including use of overhead assets, do not readily yield information concerning the function of the facility, although they may be helpful in detecting the facility and assessing the above-ground human activity associated with the facility. There is therefore a need to investigate additional techniques for characterizing UGFs.

Characterization is one aspect of the total UGF problem, which includes the following components:

- Detection
- Characterization
- Functional Kill
- Damage Assessment

Our study concentrated on technical approaches to characterization of UGFs.

Techniques for characterization can be classified into *covert* or *overt* techniques, and into techniques that can be used at *standoff* range (> 1 km) (contrasted with those methods that can be used only in-close to the facility). Our study concentrated on covert emplaced sensors and on techniques that could be used at standoff distances, e.g. on a high-altitude unattended air vehicle (UAV) or in near-earth orbit.

The problem of the detection and characterization of UGFs has been well-studied. Several excellent reports and summaries have been written on the problem [1, 2, 4, 5]. There have also been several JASON studies that relate to UGFs, including an earlier study on detection and characterization of underground structures [6], and a study on the role of unattended ground sensors in characterizing proliferation activities.

The conclusion of most of these studies is that the UGF problem must be approached using a wide range of information sources, including both technical approaches and human intelligence (humint). Fusing the information from these many sources is an important aspect of the total problem — the critical information is often buried in a few places amongst a much larger quantity of information, and no one piece of information by itself is unambiguous. An oft-used cliche (appearing in almost every report) is that there are "no silver bullets" in the UGF problem.

Realizing that the UGF problem has been extensively studied in recent years, we undertook a study at DARPA's request to look for new opportunities for progress in the detection and characterization of UGFs. Part of our charge was to identify the most promising technology areas for investment, emphasizing standoff and covert sensor techniques. Our study therefore surveyed a wide range of approaches, and we received numerous briefings. These included summaries of the technology programs of various agencies and briefings from organizations and companies on specific technology approaches. In

addition various new ideas were suggested by JASON contributors. The approaches we considered included:

- Imagery & Change Detection (Visible, IR, and SAR)
- Power Line Monitoring
- Spectroscopy (Visible, IR)
- Vibration Sensing (Man-made sources)
- Detection of Chemical and Biological Signatures
- Detection of Low-Frequency Electromagnetic Emission from Man-made Sources
- Seismic Imaging (Active and Passive)
- Gravimetry
- Low-Frequency EM Induction (Resistivity mapping)

In Table 1.1 we give a summary "scorecard" for these methods. For each approach Table 1.1 gives the type of information (characterization ability) yielded by the approach, whether the approach can be implemented in a standoff mode, whether the approach is covert, and our summary judgment on the promise of the approach.

Table 1.1

Method	Characterization Ability	Standoff?	Covert?	Outlook
Imagery/ Change Detection	Adits, Shape	Aircraft/Satellite	Yes	Promising
Power Lines	Machinery current/voltage	~100 m	Yes	Promising
Spectroscopy (Fraunhofer, etc.)	Effluents; Nuclear	Aircraft/Satellite	Yes	Promising
Vibration Sensing	Presence/Location of machine	Laser: Aircraft/Satellite Geophone: $\leq$ 1 km	Yes	Promising
Chem/Bio Sensors	Chem/bio signatures	No	Maybe	Promising
Passive EM	Location of machinery	$\sim$ km	Yes	Uncertain
Passive Seismic Imaging	Size, Shape	~100 m	Yes	Uncertain
Active Seismic Imaging	Size, Shape	~100 m	No	Uncertain
EM Induction	Size, Shape	No	Maybe	Not promising
Gravity Gradiometer	Size, Shape	~100 m	Maybe	Uncertain

Our overall conclusion is that standoff methods are feasible but technically challenging. In contrast, emplaced detectors are becoming more attractive with improvements in electronics, sensors, and communications technology, and thus emplaced sensors offer a large potential payoff. Our conclusions are:

- Standoff Methods
  - Standoff methods are feasible but mostly difficult
  - Possible standoff methods include:
    * SAR Change Detection
    * Fraunhofer Imaging (Hyperspectral)
    * Laser Vibrometry
- Emplaced Sensors
  - Sensors include: acoustics, vibration sensing, seismics, imaging, powerlines, EM emissions, chemical and biological signatures
  - Technology investment: covert communications, power systems, precision placement, miniaturization

2 TECHNICAL APPROACHES TO CHARACTERIZATION

2.1 Vibration Sensing/Seismics

"Listening" to UGFs has a certain appeal. Eavesdropping on a facility, both during construction and during operation might yield a wealth of highly specific information: location of digging operations and therefore the geometry of the facility, or existence and location of critical infrastructure such as pumps and generators. Listening might also provide information on human activity such as operation of elevators and transport equipment.

Geophones are the conventional detector used by the seismic research community and seismic exploration industry. These devices are simple, yet remarkably sensitive, with sensitivity of –50 dB $(\mu m/s)^2$ Hz in the frequency range 10–100 Hz.

Efforts are underway to determine the feasibility of *remote* sensing of acoustic vibrations (e.g. Berni, 1994) [3]. These efforts typically involve illuminating some surface with a coherent laser beam and looking for modulation of the return signal at acoustic frequencies by surface vibrations. As part of this study, we investigated such techniques and suggest possible refinements and variants.

A key issue for vibrations sensing is the ability to localize a source by using "triangulation". The characterization value of vibration sensing is enhanced enormously. For instance, while the detection of the spectral signature of an exhaust fan is of little value in itself, the localization of the fan may yield information on the location of ducts and adits which are vulnerable to attack.

In Section 2.1.1 we discuss vibration monitoring and how it might be used to detect, characterize, and localize machinery and other sources of acoustic frequency vibration from UGFs. We also comment on possibilities for imaging of UGF structures using ambient seismic waves. In Section 2.1.2, we discuss basic noise and signal levels and the resulting sensitivity for detection. Possibilities for standoff sensing of vibrations using laser vibrometry is discussed in Sections 2.1.3 and 2.1.4.

2.1.1 Applications of acoustic and seismic sensors

Passive Listening and Localization of Man-made Sources

Passive recording of vibrations or seismic signals is useful for monitoring activities during the construction and use of a UGF; such signals may also be useful for determining whether countermeasures have been effective or not. A source can be characterized by some combination of its frequency spectrum, temporal pattern and location. Many pieces of machinery have characteristic spectra that are unique enough for identification. Once a particular signal has been identified above the noise level, recordings from a minimum of 3 sensors are required in order to triangulate to the source location. As described below, however, there are great advantages to employing far more than 3 sensors. The spectral range likely to be of greatest interest for monitoring activities and machinery is between $\sim$ 10 and 250 Hz. Corresponding wavelengths are of the order of 2-50 m and 20-500 m in unconsolidated sediments (soils) and solid rock, respectively (wave velocities of order 500 m/s and 5000 m/s). Assuming a quality factor as low as Q $\sim$ 10-30, typical of the Earth's surface, means that sensors must be within about 20-60 m and 200-600 m of a source, for soil and rock, in order to obtain reliable records at the highest frequencies. Although it might be possible to localize a point source to better than about 1 wavelength's distance using phase coherent processing, there is a distinct advantage to emphasizing the

highest-frequency waves ($\sim$ 2-5 m and 20-50 m resolution at 100-250 Hz in soil and rock respectively). Of course, these are also the most rapidly attenuated frequencies, so a sensor separation of less than 40-120 m and 400-1200 m is optimal for soil and rock, respectively. In general, the horizontal location of a source is more reliably determined than its vertical position, and the reliability of the location is significantly improved if the source is within the horizontal spread of the sensor array. Thus, having more than 3 sensors helps improve the determination of source location not only because of increased redundancy in the triangulation, but especially because the likelihood of the source being within the array is increased. In particular, without detailed prior knowledge of the 3-dimensional velocity structure underground, it only becomes practical to identify and begin to account for heterogeneity in wave velocities (i.e. complications in the geology) underground if the source is located within the horizontal extent of the array. It is necessary to account for velocity heterogeneity in order to have reliable source locations, especially in the vertical.

Active Seismic Imaging

Active sensing, in which a source independent of the UGF is used, offers the potential of imaging the structure. The concept is identical to that traditionally used in exploration seismology, in which explosions (usually at or below the surface) or vibrating machines at the Earth's surface generate, respectively, wave fronts or wave trains that reflect and refract off the structures at depth. Resolution is again dominated by the wavelengths covered, so the numbers given above still apply.

The main advantage to the method is that it may be possible to obtain images of underground structures, yielding detailed information about shape, dimensions and depth. Given a sufficient number and spatial distribution of sources and sensors, methods akin to tomography can be used to obtain at least 2-D and perhaps partially 3-D images of the UGF. The highest-resolution images are typically obtained from reflected waves, and the velocity

structure of the rock or soil above the UGF can in principle be determined through studies of the refracted waves. Therefore, the method is intrinsically less limited than passive recording in obtaining reliable locations at depth. Moreover, the same sensors can be used for both active and passive recording.

It is difficult to imagine how this might be accomplished by covert means, however. Except under special geological circumstances, natural seismicity is unlikely to be high enough to offer the potential of imaging except, perhaps, on a timescale of years. Also, though many distant ("teleseismic") earthquakes might be recorded, the waves will likely be of too low a frequency (below 1-10 Hz) for adequate resolution.

Non-cooperative man-made sources of noise are potentially useful for seismic imaging. These include sonic-booms, detonations associated with mining activity, and the noise from large machinery and vehicles. Considerable research is needed to determine whether these can be used to help characterize the acoustic propagation environment, analagous to the problem of sound propagation in ocean acoustics.

2.1.2 Sensitivity, noise and signal levels

A standard device for sensing high frequency seismic waves in the earth is the geophone, which has a noise level of about –50 dB $(\mu\text{m/s})^2/\text{Hz}$ [3]. This compares to ambient seismic noise levels of between –40 dB and –80 dB $(\mu\text{m/s})^2/\text{Hz}$ in the 10-100 Hz regime depending on the location and geology.

While geophone performance is impressive, such sensitivity is needed for detection of the small acoustic signals from buried facilities. The seismic wave (velocity) amplitude, A, resulting from a source putting out P watts of acoustic power is approximately:

$$A \sim 2.5\ \mu\text{m/s}\left(\frac{R}{100\ \text{m}}\right)^{-1}\left(\frac{\epsilon P}{1\ \text{W}}\right)^{1/2} e^{-\alpha_t(f)Rf/c_s}$$

where f is the acoustic frequency, R is the distance between the source and the geophone, ϵ is the coupling efficiency of the acoustic power into the earth, $\alpha_t(f)$ is the attenuation coefficient for propagation through the earth, and c_s is the sound speed (assuming spherical spreading).

The general problem of coupling and subsequent propagation of acoustic/seismic energy from mechanical sources is beyond the scope of this report. Probably the largest signal that can be anticipated would come from tunnel boring machines (TBMs). These large devices are strongly coupled to the surrounding rock and operate at megawatt power levels. Measurements, described later, of surface vibrations 50 m above an operating TBM indicate ground motions of several microns for frequencies below 100 Hz. Representative geophone data for TBM operations are shown in Figure 2-1.

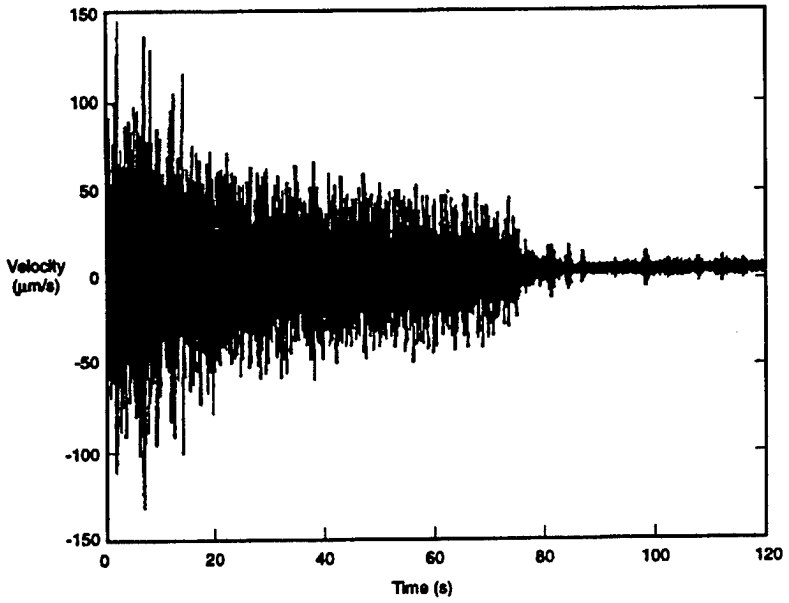

Figure 2-1: Horizontal geophone measurement on wellhead of Test Well T-8, Town Brook Tunnel Project. The TBM was shut down at about 75 seconds from the beginning of the data shown. Starting time is 00:35:03 UTC on 29 March 1995. The sampling rate has been reduced by decimation from the originally recorded rate of 12 kHz to 500 Hz.

To have a chance of detecting and characterizing underground activities during operations will undoubtedly require significantly smaller detection thresholds. As a practical matter, we suggest that geophone-level sensitivities should be the goal of any alternative development effort aimed at seismic-acoustic detection.

2.1.3 Laser vibrometry

One commonly used approach for sensing vibrations is called laser vibrometry. Laser vibrometry is a highly developed technology permitting remote sensing of vibrating surfaces over broad ranges of amplitudes and frequencies. Laser vibration sensors (LVS) employ heterodyne laser radar to extract Doppler shifts in the frequency of backscattered laser radiation, from which the speed of the vibrating surface is determined. Commercial LVS systems with resolutions in the sub-μm/s range over bandwidths of tens to hundreds of kHz are readily available.

Given its inherent sensitivity, bandwidth and demonstrated technical and commercial base, LVS presents attractive possibilities for various applications where it is impractical to implant arrays of geophones or other such seismic detectors, where large standoff distances—UAV or space-based—are required, and where flexibility in selection of monitoring points is desired. Potentially useful targets of LVS (operating within the frequency range, $0 - \text{few} \times 100\text{Hz}$) for characterizing and monitoring activity in underground structures include:

- HVAC vents
- emergency power intake and exhaust vents
- power lines and transformers
- exposed water and sewer lines

- acoustic signals on the overburden surface arising from underground machinery and activity.

The first four of these kinds of targets represent straight-forward applications of LVS technology where detectable amplitudes (1 μm/s-level) may be expected. Detecting and analyzing surface acoustic signals will likely involve much smaller amplitudes and may require arrays of target locations to reconstruct relevant direction, amplitude and frequency information. In all these cases, the "point-and-shoot" aspect of LVS can be a significant advantage.

Comparisons of LVS have been made with geophones [3]. Some of these comparisons have been at relatively short stand-off distances (1-100 m) and have used stable platforms for the laser. Such systems tend to correlate well with reference geophones for large signals. However, the sensitivity performance compared to geophones is quickly degraded by turbulence and other factors. In daylight conditions of high turbulence, noise performance can be 50-60 dB worse than for geophones [3], and even in the best turbulence conditions, the noise can be 30 dB above that for a geophone. We therefore consider conventional LVS on ground-acoustic targets to be a marginal technique and impractical for standoff characterizations of UGFs at distances greater than a fraction of a kilometer.

The ultimate performance of LVS systems is governed by factors such as laser frequency stability and fluctuations in phase and amplitude of the return signal due to laser speckle, mechanical vibrations in the LVS system, and atmospheric distortions when long path-lengths through air are employed. In bench instruments, optical fibers can be used to minimize the path-length through air while retaining flexibility for selecting the target spot. In some systems, a second fiber—the "reference" fiber, equal in delay to the signal fiber and serving the role of the local oscillator—is added to the system to permit differential vibration measurements; such reference beams naturally

circumvent or reduce certain deleterious effects on performance, such as those arising from fluctuations in laser frequency.

We received briefings and written material (some proprietary) by the Laser Systems Division of Litton Systems, Inc. The Litton group has extensive experience with LVS systems, including applications for identifying distant flying aircraft based on characteristic vibration signatures. They have performed proof-of-principle tests measuring seismic vibrations in the vicinity of a tunnel-boring operation and vibrations on an above-ground exhaust stack serving underground electric generators. The tunnel-boring results appear to correlate well with corresponding geophone data, such as data presented above in Figure 2-1. The Litton group also presented us their reports on the feasibility of space-based LVS and on issues related to seismic directional processing. We are favorably impressed by this body of work.

The Litton studies consider three potential lasers, Nd:YAG ($\lambda = 1.064\mu$m), Ho-Tm:YAG ($\lambda = 2.091\mu$m), and $C^{(18)}O_2$ ($\lambda = 9.115\mu$m). Their trade studies—examining different standoff distances (few $\times$ 100 m to few $\times$100 km), laser power levels, apertures, atmospheric conditions and CW/pulsed operating modes (potentially important for reducing effects of speckle noise when the relative transverse target/LVS velocity is large)—yield expectations for broadband sensor output noise below 1 $(\mu\text{m/s})/\sqrt{\text{Hz}}$ (discrete frequency output noise $< 1(\mu$m/s) rms) for reasonable values of operating parameters.

Litton's "proof-of-principle" experiments had LVS signals (for frequencies in the range 10–100 Hz) greater than the noises quoted above. Taken together with scaling arguments, these measurements led the Litton group to suggest the feasibility of UAV and space-based LVS operations for certain kinds of underground targets. The exhaust stack measurement represents a classic use of LVS that may not be available in a well hidden underground facility. The tunnel-boring study clearly detects surface acoustic signals from a tunnel-boring machine (TBM) operating about 50 m below the surface. It should be noted that TBMs are large (3.4 m diameter by $>$ 10 m long, in the

case studied) and noisy (the TBM detected operates at 1 MW); machinery involved in normal operations within an underground structure—elevators, fans, machine tools—are likely to yield much smaller surface acoustic signals. As emphasized by the Litton group, monitoring of surface acoustic signals also presents new data-handling challenges because the target area will likely be larger than the laser beam spot, with its own complicated wave patterns that must be analyzed to interpret the underground source. Exhaust stack-type measurements can be performed with laser beam spots of roughly 1 m (radius), as would be expected for the wavelengths, LVS apertures, and standoff distances contemplated. To go beyond TBM detection or well-coupled-exhaust-stack monitoring, it will be necessary to push the state-of-art in sensor noise levels below the 1 $(\mu\text{m/s})/\sqrt{\text{Hz}}$ level. It may also be necessary to employ arrays of reflectors coupled to the ground. Even with arrays giving many reflection points, atmospheric turbulence presents formidable challenges for any remote-sensing version of LVs.

2.1.4 Areas for possible improvements in LVS

Use of corner-cube retroflectors

One approach where we encourage additional effort is the use of corner-cube retroflectors (CCR) in long-standoff applications of LVS. The advantages of using CCRs are:

1. Increased return signal per unit target area
2. Elimination of target speckle.

The main disadvantage of CCRs is that they must be mounted on the target surface, which may be difficult if access is limited or denied. In cases where covert monitoring is required, discovery of the CCR would be a tip-off of the LVS operation. However, rather small CCRs (millimeters in size), coated

to reflect only the wavelength of interest and otherwise camouflaged, could be air-dropped or surreptitiously placed for acoustic/seismic monitoring in remote areas with little chance of detection. It should be relatively simple to deploy arrays of such CCRs to permit reconstruction of acoustic LVS information over large-area targets. Coupling of CCRs to the surface is a particular issue in LVS, but should be possible, even when being placed remotely, using various mechanical or gluing techniques.

The linear dimension of the CCR must be chosen large enough for the specularly reflected power at the detector will exceed that from the Lambertian reflection of the laser beam spot. Assuming the Lambertian reflectance, ρ, of the underlying target surface is uniform over the laser beam spot, this condition on the CCR size, c, is:

$$c > \lambda \left(\frac{\rho}{2\pi \cos\theta} \right)^{1/4} \sqrt{R/D}$$

where λ is the wavelength of the laser radiation, θ is the angle between the laser beam direction and the normal to the target surface, R is the range from the LVS source to the target, and D is the LVS aperture. The reflectance of the CCR is assumed to be unity. Even for space-based applications, CCRs of a few mm to a centimeter should be adequate.

Differential LVS By themselves, CCRs can eliminate speckle noise, but we see them as providing greater benefit if used in pairs, one coupled to the ground and one isolated or "inertial", to provide a ground-level phase reference that can substantially reduce noise arising from fluctuations in laser frequency and atmospheric distortions. This approach is similar in concept to differential LVS employed in laboratory instruments, but, to minimize atmospheric disturbance, the two targets should be placed close together, meaning that, as a practical matter, both targets will share the same laser footprint. One must then sort out the differential phases in the same return beam.

One way to accomplish differential LVS, using polarization to distin-

guish the two retroflectors, has been demonstrated over a 200 m standoff distance [3]. In these experiments, one polarization interrogated one retroflector acoustically coupled to the ground, the second reflected from a retroflector that was isolated from ground vibrations—the inertial reflector—for the frequencies of interest and a reference geophone was mounted onto the same target package, shown in Figure 2-2. The noise level was 15 dB higher than for a geophone under low turbulence conditions, and about 30 dB worse for high turbulence conditions, as shown in Figure 2-3.

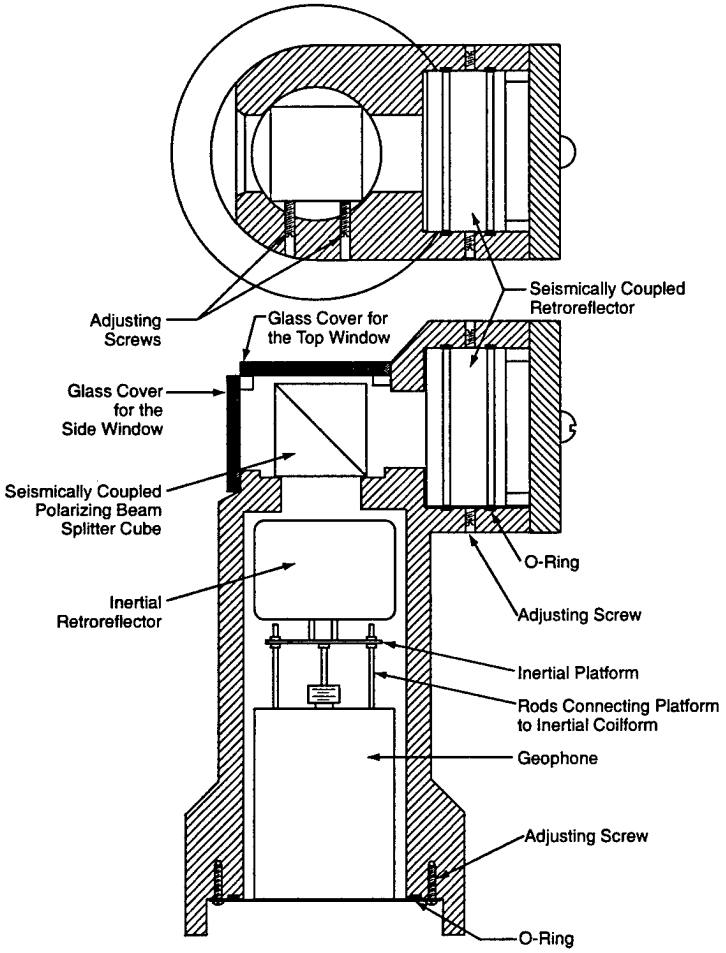

Figure 2-2: Cutaway drawing of the retrophone.

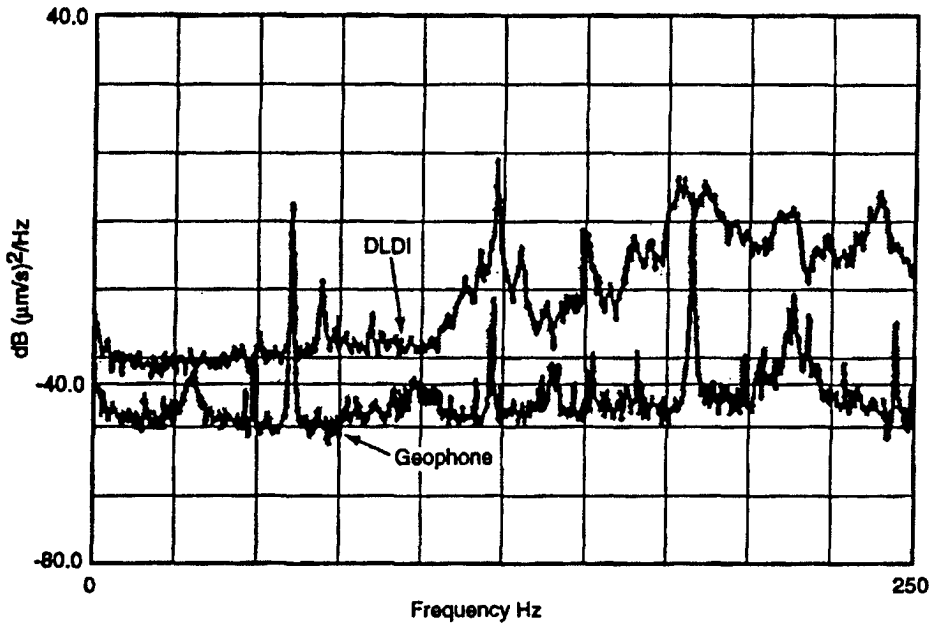

Figure 2-3: Noise spectral comparison between retrophone (upper curve) and geophone (lower curve). Complete turbulence cancellation is achieved and the electronic noise of the DLDI receiver is reached in this nightime test. The geophone is also limited by its electronic noise floor, which in this case is the electronic noise of the DFSV recording system.

We have also considered a different approach to differential LVS using a pair of acoustically independent CCRs placed adjacent to each other in the same laser beam, but without using polarization information. In this case, if one CCR is displaced, interference fringes will "sweep" past the receiver in proportion to the path difference between the two CCRs, resulting in an amplitude modulation at the receiver. One possibility for reducing the potentially large AM noise in such a setup would be to use a pair of adjacent receiver apertures to "count fringes" in the returning beam. The magnitude of the receiver asymmetry (difference in power divided by sum) will be related to the magnitude of ground motion, the time-dependence of the receiver

asymmetry is related to the time dependence of the ground motion, and the total return power can be used to track the laser beam on target.

We suspect that differential LVS using the polarization information will turn out to be the preferred approach. In any event, differential LVS looks promising for achieving sensitivities of interest in monitoring acoustic signals from underground sources. The main disadvantage is that a target must be placed on the ground. Either approach can probably be accomplished with relatively simple, small, and inexpensive targets, but work will be needed to develop and camouflage them. We feel that the potential payoff of differential LVS justifies an investment in appropriate target R&D. We note, however, that if one is willing to accept ground-implanted targets, an even better acoustic detector would be geophones equipped with a simple data exfiltration device, such as a modulated CCR. These should also be studied. A choice could then be made between the geophone approach, presumably offering superior performance, but requiring a power source, and LVS using a pair of CCRs, that would not need power on the ground.

2.2 Power Lines

Detection and tapping of power lines is a promising approach for characterization of UGFs. Power lines are part of the power infrastructure of most underground facilities and are one of the obvious targets to attack as one component of functional defeat. In addition, power lines can provide important information about the facility.

Exploitation of power lines first requires their detection. We were briefed on airborne 3-component magnetic field sensors used to map large power grids. These sensors detect the magnetic fields from the unbalanced currents in the lines. They have a sensitivity of 5×10^{-14} T/Hz$^{1/2}$, have 5 m surface resolution at 100 m altitude, can detect power lines up to 40 km, and to a

depth of 100 m below the earth. Such a package could be flown on a UAV or carried in a land vehicle to locate power lines that may be associated with a UGF. A key goal of mapping of field lines would be to identify electrical substations that are in the network that supplies power to the UGF.

Once found, small, inconspicuous sensors can be attached to or placed near the power lines. These sensors can be emplaced on cables, insulators, or towers and can be powered by ambient fields. They can be readout by RF link, RF transponder, or possibly by modulated reflection of a laser. Once emplaced the sensors can monitor:

- Current. Current monitoring provides information on activity/usage patterns.
- Voltage and Current Waveform Distortions. Waveforms can provide information on the nature of equipment including power switching systems, rectifiers, etc.
- Outgoing Signals. Power lines can be used for communication, i.e. exfiltration of signals.

Remote readout of emplaced sensors appears to be the most straightforward approach to monitoring power lines. We also thought about possibilities for standoff sensing of power lines ($\geq$100 km) in those cases where emplaced sensors are not feasible. We suggest the following approaches, recognizing that considerable work would be required to demonstrate feasibility:

- Voltage Waveform Monitoring. Corona discharge will produce RF emission which may be detectable. This effect would be weather dependent.
- Current Monitoring. Generation of magnetic fields by unbalanced currents can lead to vibrations of cables and towers which might be detectable as modulation in the return from radar signals. These vibra-

tions could be a large as 10^{-3} to 10^{-1} cm in amplitude. Simple ground based radar experiments could test the feasibility of this approach.

2.3 Imaging & Change Detection

Imaging at optical, IR, or radio wavelengths is a primary method of obtaining information for the characterization of underground facilities. Imagery can yield information about the nature and scope of above-ground activity, and can sometimes be used to detect tell-tale signs of UGF construction: mine tailings, adits, power lines, etc.

Change detection is an even more powerful tool for characterization. At optical and IR wavelengths, change detection can reveal road and above-surface building construction, as well as changes in soil and rock composition, excavations, etc. Change detection at radio wavelengths can be even more powerful allowing the detection of ducts and adits, slumping of ground, presence of tailings, etc.

During this study, we concentrated primarily on the use of SAR for characterization of UGFs. In Section 2.3.1 we discuss how SAR can be used to detects adits, pipes, and other openings. Section 2.3.2 discusses detection of ground settlement due to underground construction.

2.3.1 Matched filter SAR for adits

When viewing SAR images, numerous artifacts occur in the image such as adits, wires, pipes, and openings into structures, delay and reflect back SAR signals differently from the simple scattering model assumed by the usual SAR image forming algorithms. If a SAR signal propagates down an adit, tunnel, or hallway in a building, it will be reflected and delayed.

The resulting artifact can help identify and characterize this feature in the observed terrain. The problem of discovering adits, etc., however is still difficult because this artifact is not an intense point, but rather a smeared out pattern that depends upon a lot of factors of the observation as well as the adit structure. What is needed is a SAR processing algorithm that is matched to adits, etc., so that a bright and focused spot will mark the adit upon a "smeared out" image of the ground, i.e. a matched filter algorithm.

Formulation of the "Adit Matched Filter"

The signal received by a SAR platform distance along a track that lies in the y-direction is

$$R(t,u) = \int_{x,y} \frac{1}{d^2}\sigma(x,y)\ \delta\ \left(t - \frac{2d(u,x,y)}{c}\right)$$

where

$$\begin{aligned} t &= \text{time} \\ \sigma &= \text{radar cross section} \\ c &= \text{speed of light} \\ d &= \text{distance from patch at } (x,y) \\ u &= \text{platform position in } y\text{-direction} \\ h &= \text{platform altitude} \\ d &= \sqrt{h^2 + x^2 + (y-u)^2} \\ \delta(0) &= 1;\ \delta(t) = 0 \text{ if } t \neq 0. \end{aligned}$$

The transmitter waveform is assumed to have an autocorrelation function that is, for all practical purposes, a delta function $\delta(0)$.

It was shown in the JASON report "SAR" (JSR-93-170) that the above formula can be inverted as

$$\sigma(x,y) = k \int_t \int_u R(t,u) f = \phi\left(t - \frac{2d(u,x,y)}{c}\right)$$

where $f = \phi(k)$ is the discrete "Mexican hat function"

$$\begin{aligned} \phi(0) &= \pi^3 \\ \phi(k) &= -k^{-2} \quad \text{if} \quad k \neq 0. \end{aligned}$$

To design the matched filter we simply modify the SAR image formation by increasing the returned time by ΔT, the assumed depth of the adit. The ϕ function is then

$$\phi\left(t - \frac{2d(u,x,y)}{c} - 2\Delta T\right)$$

where ΔT is the one-way time it takes the radar signal to traverse the adit. The depth of the adit is then

$$d_a = \Delta T\, c.$$

Computer Simulation

To illustrate these concepts, a simple computer simulation of the SAR receive process and the SAR image formation process was created. In the above formulas discrete sums replace the integrals. The complete simulation program written in the 'C' language is attached.

Results

Figure 2-4 illustrates the signals received from four targets. The first target is at the ground level. It produces a returned signal highlighted in orange color. The signal strength is represented as a single digit at the track location and time it is received.

The second signal, highlighted in red, is the same return but delayed by its traverse of the simulated adit. The next two signals in green and yellow are targets at ground level adjusted in the x-direction to match the adit return at its ends and at its middle. They illustrate that a return signal from the adit is not the same as a displaced target signal. The adit signal will be unique and detectable by the matched filter.

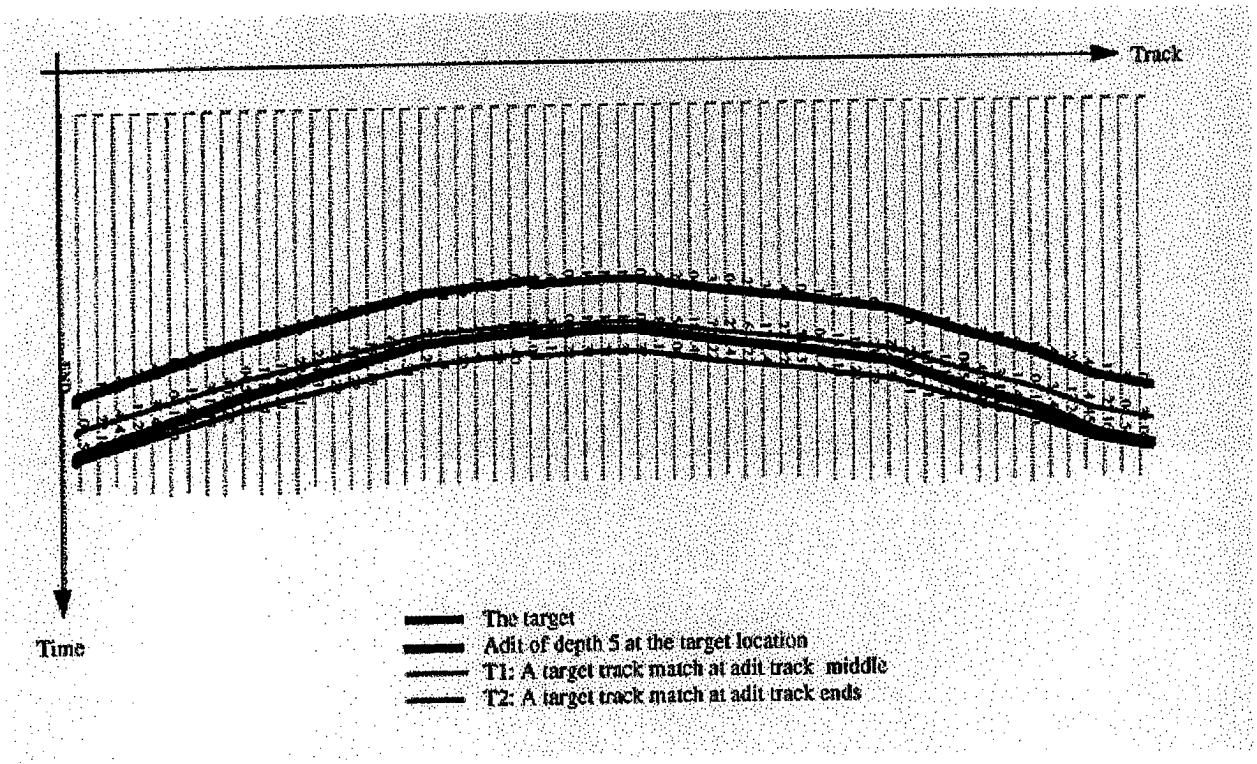

Figure 2-4: Simulation of SAR return signal.

Figure 2-5 illustrates the matched filtering and the usual image formation processing of the target and adit signals. Here there is a simple ground target and an adit at the same ground location. If the matched filter is employed, the target displays as a tiny residue whereas the adit produces a strong response. If the usual image processing is employed, the target gives a strong response, but the adit only produces a "smeared out" residual.

Depth Algorithm

To detect adits over a range of depths, the original received SAR signal must be processed repeatedly over the range of the depths. Then each image path at a given location must be examined to determine if a strong response occurs for any of the depths. Figure 2-6 illustrates this. If a peak in response

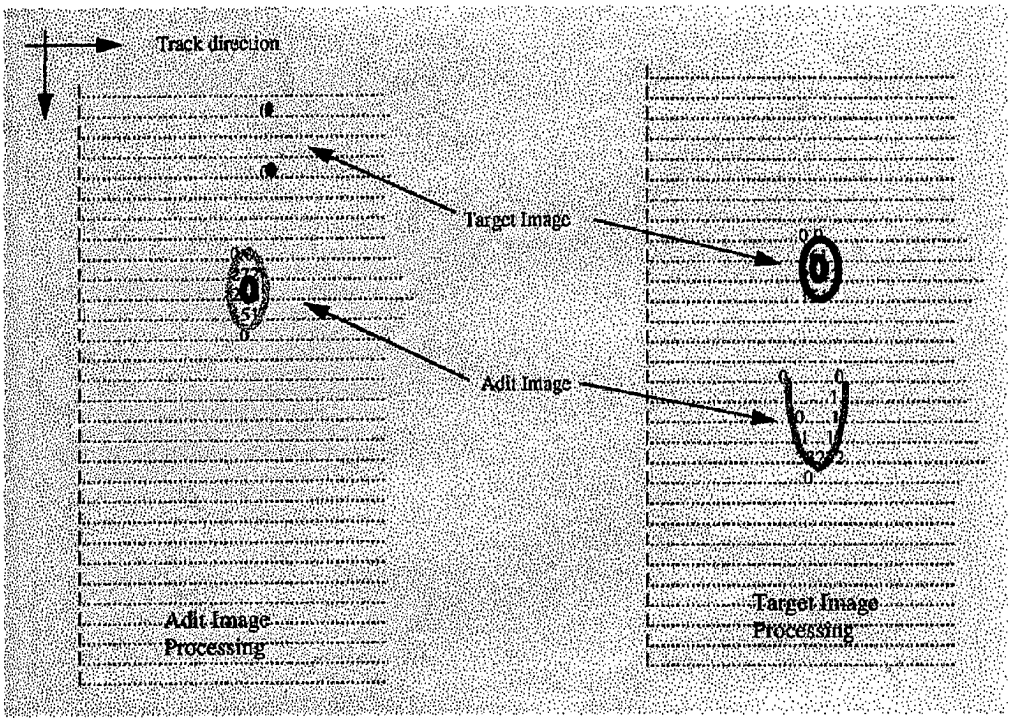

Figure 2-5: Calculated SAR images.

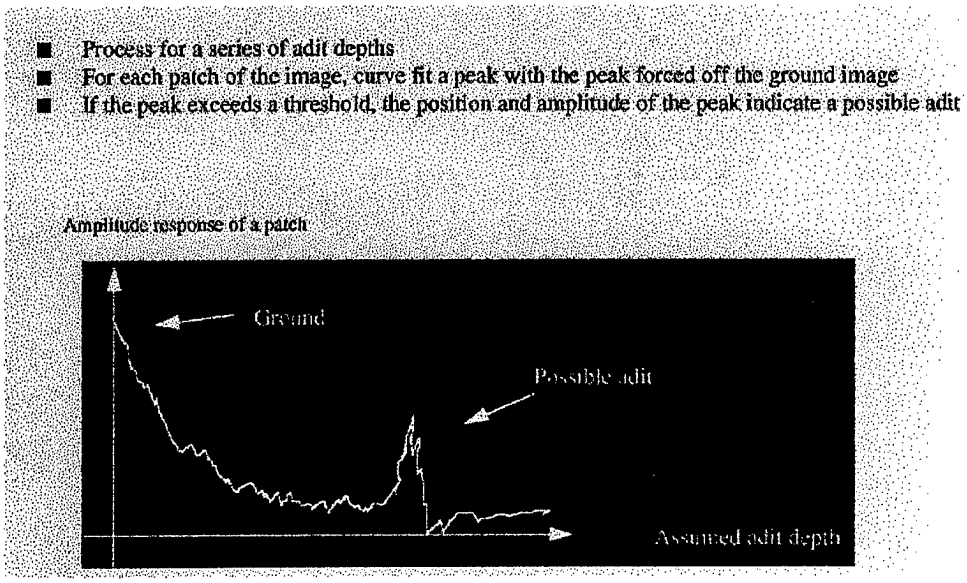

Figure 2-6: Depth algorithm.

outside of the ground response at $\Delta T = 0$ is found, then there is evidence for an adit at that location and depth.

Conclusions

SAR observations and processing have been previously employed to characterize artifacts discovered in SAR images. However, to avoid having the "image" of the artifact smeared out and lost, the SAR observations are chosen to occur at low angles and at a long distance that results in large "f-number" imaging (small synthetic aperture relative to range).

The goal here is to distinguish adits from ground clutter so we want just the opposite: small "f-number" imaging. Thus we want very wide synthetic apertures taken near the ground at high aspect angle.

It will be useful to process multiple images of the same ground but with a diversity of views. This should greatly increase the adit detection sensitivity.

The next step in evaluating the matched filter idea is to try the matched filter algorithm on actual SAR raw data.

2.3.2 SAR detection of ground settlement due to underground construction

Settlement of the terrain surface due to underground construction beneath is well known in civil engineering [8] p.91. It is a constant worry because settlement can damage structures above the underground construction and particularly on the surface. The surface settlement for underground structures above basement rock and within a few to a few tens of meters of the surface is substantial, depending on the type of soil. For example, pipeline tunnels of a few meters in diameter at depths of a few to a few tens

of meters cause settlements with a maximum of 1 to 10 cm directly over the tunnel and lesser settlement distributed over a surface distance of a few tens of meters transverse to the line of the tunnel. A typical example is shown in Figure 2-7 below.

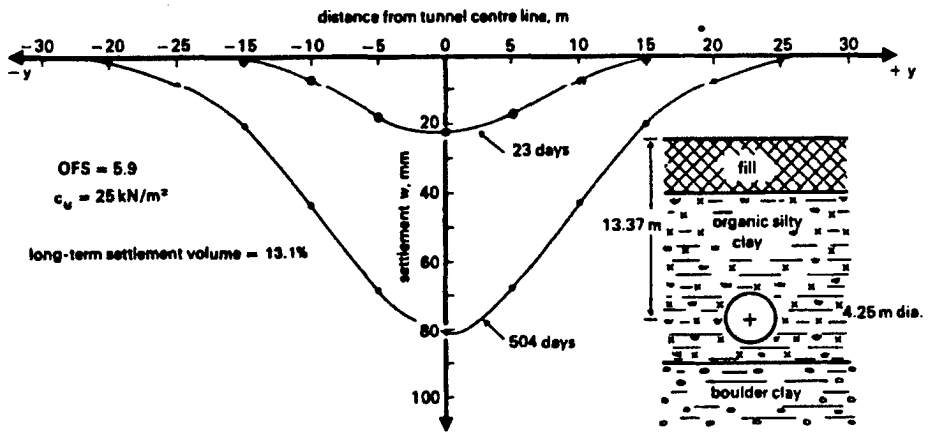

Figure 2-7: Distribution of surface settlement over distance traverse to the line of the tunnel. After Attewell et al. (1986)

In addition to the vertical settlement at the surface there is also a horizontal straining of the surface. Both of these effects, settlement and surface straining, impact both the surface itself and any structures on the surface. The impact on structures (tilting, cracks or more serious structural damage) is the reason that surface settlement due to underground construction has been so thoroughly studied by civil engineers.

The physical mechanism for surface settlement is that an "excess volume" is removed during tunnel construction, typically $\approx$ 10% of the tunnel volume for pipeline tunnels. As time passes, this void propagates upward to the surface and produces a settlement trough affecting a width 5 to 10

times the tunnel diameter. As an example, the maximum depth of the settlement trough for the 4.25 m diameter tunnel at 13.4 m depth in clay soil at Willington Quay, UK (Figure 2-7) was 2.2 cm after 23 days, increasing to 8 cm after 504 days. Since the depth of such settlement troughs is typically greater than a wavelength for X-band (3 cm wavelength) radars, they should be detectable using radar techniques.

Synthetic aperture radar (SAR), in particular, interferometric SAR (IFSAR) provides an excellent way to detect the presence of underground structures as revealed by surface settlement and/or straining. The idea here is to collect two (or more) complex SAR images of a site and compare the complex amplitudes of the corresponding pixels in the two images. Clearly the two images must be collected with the same observational geometry or corrected to be as if the observational geometry were constant for the two observations. The two images should be collected before and after the settlement takes place, say a month or more apart. However, as noted above, settlement continues over months to more than a year. So the complex SAR images could be collected at rather flexible times and still be meaningful – even after the underground construction takes place. Settlement might also be detected by movement of buildings that are over the settlement area.

Typically synthetic aperture radar (SAR) images are, like photographic images, intensity images corresponding to the magnitude squared of the received signal. Unlike photographic images, SAR images can be complex, contain both amplitude and phase information for each pixel. Suppose we form the complex cross correlation coefficient for each pair of registered pixels, collected at times t_1 and t_2, and average over a block of a few tens of pixels, namely $< s_1 s_2* > / < [(s_1 s_1*)(s_2 s_2*)] > = \mathrm{M} \exp [\mathrm{i} (\phi_1 - \phi_2)]$. We now have an image where each pixel is a measure of the phase difference between a pixel from the image at time t_1 and the corresponding pixel from the image at time t_2. The complex SAR images collected at separate times over a given site need to be registered to high accuracy or significant noise will be introduced. Because of averaging the resolution of the phase differ-

ence image is usually a factor of 2 to 10 worse than the original complex image data. If the surface is unchanged between times t_1 and t_2, the phase difference $(\phi_1 - \phi_2)$ will be zero because the phase path of the radar waves is the same for both cases, i.e. both images were collected from the same observational geometry (or effectively so). If the surface has moved due to settlement, corresponding pixels will have a phase difference. The resulting image will then have phase difference fringes on it corresponding to the structure of the settlement. This technique was used on a larger scale to detect the ground movement caused by an earthquake near Landers, California as shown in Figure 2-8 [9]. In this case the two complex SAR images were collected by the C-band SAR sensor aboard the ERS-1 satellite from two orbits along nearly the same path, but at times separated by several months.

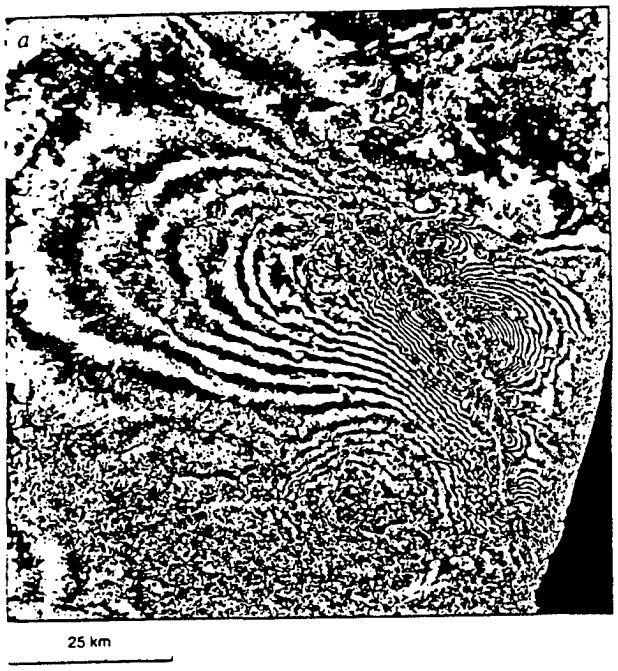

Figure 2-8: Fringe map of phase difference resulting from the Landers, California earthquake. Each cycle of phase change is equivalent to 28 mm of earth movement along the range direction of the radar. Note how the fringes are close together near the epicenter of the earthquake, center right, where the earth surface movement was greatest. After Massonnet et.al. (1993).

2.4 Low Frequency Electromagnetic Techniques

We were briefed on an active Very Low Frequency (VLF) electromagnetic approach by representatives of Advanced Power Technologies, Inc. The idea here is to map out and search for anomalies in subsurface conductivity in suspect regions. This tactic was tested experimentally on a segment of the SSC tunnel in Texas, using a local, ground-based radiation source and detectors. The tunnel showed up well in the data, at the right horizontal location and roughly the right depth. Accurate determination of depth requires the use of a wider range of frequencies than was employed in this initial round of experiments. A mine tunnel in Alaska was similarly detected successfully. Magnetic perturbations were picked up with local detectors placed above a segment of the mine shaft, as at the SSC. However, in the Alaskan mine, the VLF source was far off and ingenious. It was a purposely disturbed piece of the ionosphere. An upward-directed RF beam, operating at a frequency (2.85 MHz) chosen for strong absorption in the ionosphere, was modulated over a range of low frequencies. The beam modulates ionospheric conductivity in the affected volume, a portion of the polar electrojet; see Figure 2-9.

This region of the ionosphere near the magnetic pole is an important source of the magnetic noise that is transported through the ionospheric waveguide, which consists of the ionosphere and the earth's surface. The ionospheric modulation in effect produces a deliberate, periodic noise signal. The concept is intriguing, but much remains to be studied and tested.

There is considerable experience in the oil and mineral exploration business which demonstrates that low frequency electromagnetic radiation can be used to find underground structures. When the goal is finding tunnels, caves and the like from the surface, experience in this business is that a structure can be "seen" up to a distance of about 3 times its diameter if it is at most a few times the electromagnetc skin depth (δ) away from the source of the radiation, which usually means below the surface. Since the skin depth δ in

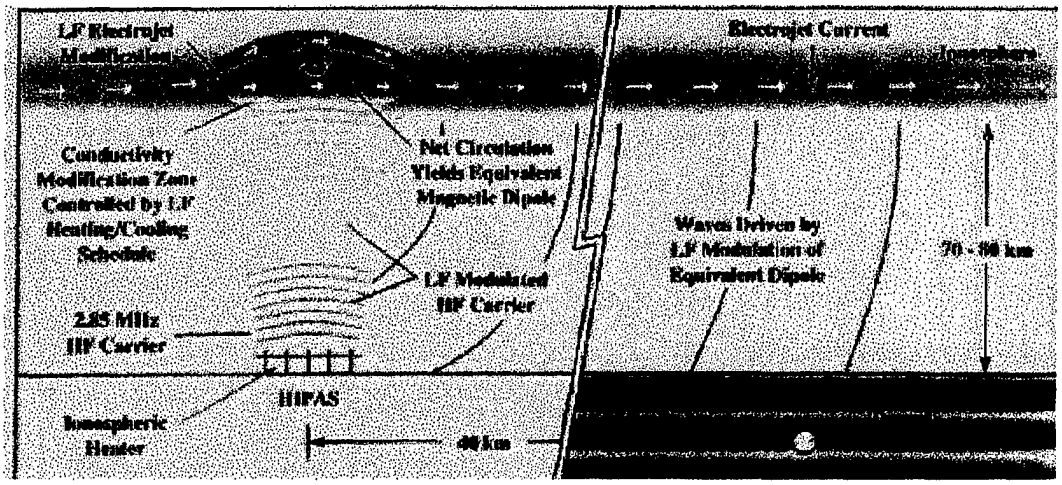

Figure 2-9: GGT schematic.

meters is given by 500 $\sqrt{\rho/f}$, where f is the frequency of the radiation (Hz), and ρ is the resistivity of the overlying/surrounding soil and/or rock (Ω-m), for any given overlayer, the benefit of using low frequency is evident. To be detectible, the structure must have a resistivity different from the surrounding material so that the oscillating electric dipole moment induced by the incident electromagnetic wave at the structure is detectible at the surface. Detection of a structure within an overlayer with a complicated resistivity profile is considerably more difficult. Clearly, mapping a "relatively deep" structure (diameter small compared to depth) with any fidelity is much more difficult than simply detecting it, especially in a complicated overlayer.

Representatives of Advanced Power Technnologies, Inc. (APTI) described a method to us by which they believe that a factor of two or three improvement can be achieved in the depth-to-diameter ratio at which a relatively deep (as defined above) tunnel can be detected. As we understand it, their principal improvement on standard methods is the use of a new signal processing algorithm that is specifically developed for finding underground structures with the use of $\approx$ 100 different illumination frequencies that range

over two decades ($\approx$ 0.5–50 kHz) or more in order to be able to cope with a range of resistivities in the overlayer. APTI's present work is supported by the Air Force. While this is a work-in-progress, we saw some interesting results of applying the method to "finding" known tunnels.

One demonstration that we saw was the location of an abandoned 2.5 m diameter mining tunnel that was 25 m below the ground in Alaska and entirely within a uniform resistivity ($\sim$ 1000 Ω-m) granodiorite layer. The frequency range used to locate this tunnel was 800 Hz to 12 kHz. The explanation for the precision with which the tunnel depth was determined (essentially exactly right), was said to be the uniformity of the rock above, around and below the tunnel in question. We wonder if the specific image of the tunnel we were shown was simply indicative of the resolution of the method in this case: a detector was placed on the ground to take data at points 4 meters apart along a line perpendicular to the tunnel axis, and the source waves were aligned to generate an electric dipole oriented perpendicular to the tunnel. Does the inversion algorithm simply locate the centroid of the electric dipole in this case? We also wonder if the fact that the skin depth for the electromagnetic waves was greater than the depth of the tunnel in this case had much of an effect on the precision.

The second demonstration presented involved "finding" the 5 m diameter tunnel built in Texas for the Superconducting Super Collider (SSC). This tunnel is 55-60 m below the surface at the test location. It is near a chalk-shale boundary, representing a resistivity change from 30 Ω-m above the boundary (in the chalk) to less than 10 Ω-m below it (in the shale). In a preliminary test run in 1995, the tunnel depth was "found" rather precisely. In a very recent run, a preliminary unfold of the data does not look so encouraging with regard to determining the depth of the tunnel. However, optimization of the unfolding of the data is still in progress.

The APTI representatives also presented arguments as to why it would be beneficial to look for tunnels if plane wave sources are applied at the surface. They then explained the operation of the HIPAS and HAARP facilities in Alaska, which generate low frequency waves by using high power few MHz radiation to modify the naturally flowing current in the ionosphere at the desired frequency. Although details on the mechanisms involved are not appropriate here, the method does generate low frequency electromagnetic waves in the waveguide consisting of the earth as one conductor and the ionosphere as the other. The wave spreads cylindrically (i.e. the wave power varies inversely as the distance) and resistive loses are very low at low frequency. Therefore, it was argued that waves launched in one of the regions of the ionosphere where currents flow, either the auroral region or the equatorial region, will be suitable plane waves a few thousand kilometers away, where a search for tunnels is to be done.

At this stage, we can say only that the new algorithm looks promising, but much more work is needed (and is in progress under the Air Force contract). In particular, there is an urgent need to test the algorithm by using it to unfold model situations. That is, computer simulated data collected by detectors on the surface above a relatively deep tunnel which is being illuminated from the surface by a specified collection of electromagnetic waves should be unfolded to see how close it matches the conditions in the model problem. Increasingly difficult model problems can be tested to exercise the algorithm and determine its limitations, as well as to guide the choice of field tests that are more difficult than finding known tunnels in known geological situations.

It is worthwhile for DARPA to monitor APTI's work on underground structure detection, but DARPA investment is not needed at present. We see two potentially serious limitations to the effectiveness of active VLF techniques. First, the imaging method appears to be very fragile in the presence of ground water or sub-surface water. Furthermore, the approach is very susceptible to countermeasures: a layer of chicken-wire placed on or immediately

below the surface would prevent imaging. Second, the method appears to require closely spaced detectors (4 m spacing was used in the experiments that were briefed to us) and these must cover the entire area above a suspected facility. Operationally this seems to be prohibitive. Regarding plane wave generation by ionospheric modification, given that the modification method works only in the auroral zones and at the equator, it is not clear that this is the best way to find structures at 30-50 degrees latitude, although the waves have very long attenuation lengths. Assuming low frequency detection works, it may be better to launch a plane wave using an array close to the area of interest. Since the detection method requires local detectors, using a locally generated known source seems perfectly reasonable.

2.5 Fluorescence & Fraunhofer

2.5.1 Passive detection of fluorescing substances in solar radiation by means of the Fraunhofer lines

Optical and infrared remote sensing methods have made use of many potential signatures, from changes in imaged features like missile silo fields, changes in color or multispectral features, which occur when vegetation is removed, shadowing under appropriate conditions of illumination, etc. Analyzing the polarization of visible or infrared light may also have some benefits to offer, although at the cost of more complicated instrumentation. Here we discuss how one might use another signature for characterizing the function of underground facilities, the remote detection fluorescence excited by ordinary sunlight.

Many chemical and biological agents, as well as spoils from excavations, have characteristic fluorescence spectra when exposed to ultraviolet and visible light. The fluorescence occurs when a photon of visible or ultraviolet

light excites a molecule, atom or ion to a higher energy level, and the excited system reemits a photon at a longer, Stokes-shifted wavelength as it makes a transition between more closely spaced energy levels than those involved in the excitation. The energy difference between the exciting photon and the emitted photon is ultimately dissipated as heat. For an efficient fluorescing material, for example, dye-like organic compounds with conjugated bonds, the quantum efficiency for fluorescence can approach 100%. Rare-earth and actinide elements, including uranium and other materials of interest to a nuclear proliferant state, can also be efficient fluorescers since they can absorb and emit light with well-shielded, inner-shell f electrons. Most materials have negligible fluorescence efficiency.

Active illumination to produce fluorescence is probably impractical except for very special cases. However, a useful part of the solar spectrum, both ultraviolet and visible, could serve as a natural source of illumination to produce fluorescence. A human obsever has difficulty perceiving fluorescence from sunlight because of the strong, normally scattered background radiation. This is why "black lights" are used for casual observation of fluorescence — for example, the simple mercury lamps with ultraviolet filters used to look for counterfeit US currency at some cash registers. However, one could detect the fluorescence with a full sunlit background by using special filters that are peaked at the Fraunhofer dark lines of the sun, wavelength bands where little light is present in the solar spectrum. An example of some of the Fraunhofer lines of the sun, taken from the McGraw-Hill Encyclopedia of Science and Technology is shown in Figure 2-10.

The Fraunhofer lines are produced by atoms or ions in the chromosphere of the sun. Since the temperature of the chromosphere is lower than that of the underlying photosphere, which can be approximated as a blackbody at a temperature of about 6000 K, much of the continuum radiation is eaten out at the centers of the Fraunhofer lines, and the lines appear as dark gaps in the solar spectrum. The strongest lines are produced by hydrogen, sodium, magnesium, silicon and iron atoms (H I, Na I, Mg I, Si I and Fe

Figure 2-10: Two selections of the Fraunhofer spectrum, showing bright continuum absorption lines. The wavelength range covered by each strip is approximately 8.5nm. The three strongest lines are produced by magnesium; the other iron.

I) along with singly ionized magnesium and calcium (Ca II and Mg II). A useful compendium of the stronger Fraunhofer lines, taken from Allen's *Astrophysical Quantities* (The Athlone Press, London, 1981), is reproduced below in Table 2.1. It can be seen that the strongest lines are typically several Angstrom units in width, and have central intensities which are typically five to ten percent of the continuum intensity. So a few percent of the visible solar spectrum and its extension into the near infrared is available for detection of fluorescence with high-efficiency, uncooled detectors like photomultiplier tubes, image-intensifier arrays, avalanche photodiodes, etc.

To roughly estimate the size of the fluorescent signal, one should imagine attenuating the ordinary optical signal of the sunlit scene by a factor of about 100 to account for the transmission of the Fraunhofer comb filter, and by a conversion factor for solar photons into fluorescent photons, which might optimistically be 1%. Thus, the fluorescent signal could optimistically be 10^4 times weaker than the ordinary sunlight signal with no fluorescence and no Fraunhofer comb filter. This could still be a very useful signal because sunlight is so intense that one can afford to use much less light, as evidenced by the success of night viewing systems.

A slightly more detailed estimate of the signal available in the Fraun-

Table 2-1: W = equivalent width, r_c = central minimum intensity corrected for instrumental distortion, c = wing intensity defined by $c = D\lambda^2(1r)/r$ [1, 9] where r is the intensity (not the depth) relative to the continuum at Dl from the line centre. The limb is represented by cos $\theta = 0.3$ where θ is angular distance from disk centre. Between cos $t = 0.3$ to 0.0 most features change rapidly.

λ	Name	Atom	Centre of disk			Limb (cos θ = 0.3)	
			W	r_c	c	W	r_c
Å			Å	%	Å²	Å	%
2795.4		Mg II	}22	10			
2802.3		Mg II		10			
2851.6		Mg I	10	10			
2881.1		Si I	2.6	20			
3581.209	N	Fe I	2.2	3			
3734.874	M	Fe I	3.1	1			
3820.436	L	Fe I	1.8	2			
3933.682	K	Ca II	19.2	3.9	39	16	8
3968.492	H	Ca II	14.4	4.1	26	12	8
4045.825		Fe I	1.2	2	0.22	1.4	5
4101.748	h, Hδ	H I	3.4	19		1.2	31
4226.740	g	Ca I	1.5	2.4	0.23	1.5	4
4340.475	G′, Hγ	H I	3.5	17		1.2	26
4383.557	d	Fe I	1.1	3		1.1	5
4861.342	F, Hβ	H I	4.2	14		1.4	22
5167.327	b_4	Mg I	0.9	12	0.09	0.7	18
5172.698	b_2	Mg I	1.3	8	0.24	1.2	11
5183.619	b_1	Mg I	1.6	7	0.37	1.5	11
5889.973	D_2	Na I	0.77	4.2	0.095	0.76	6
5895.940	D_1	Na I	0.57	4.8	0.049	0.56	6
6562.808	C, Hα	H I	4.1	16		1.4	23
8498.062		Ca II	1.3	30	0.3	1.1	32
8542.144		Ca II	3.6	19	2.4	2.9	20
8662.170		Ca II	2.7	21	1.2	2.2	22
10049.27	Pδ	H I	1.6	79			
10938.10	Pγ	H I	2.2	73		1.0	82
12818.23	Pβ	H I	4.2	63			

hofer lines can be obtained as follows. At mid day, about one kilowatt per square meter of sunlight falls on the surface of the earth. Of this, perhaps half is available in the visible, near infrared and near ultraviolet spectral regions where strong Fraunhofer lines are located. One watt of such light is about 2×10^{18} photons per second, so the incident photon flux is about 10^{21} photons/m^2. Suppose the ground is contaminated with a fluoresecent material with intercepts about 1% of the incident photons and converts them into fluorescent light. About 1% of the fluorescent light can be detected through a comb filter for the Fraunhofer lines, leaving about 10^{17} photons/m^2 available for collection with appropriate optics. For a satellite with a collection

aperture 1 m in diameter and at an altitude of 200 km, the solid angle subtended from a spot on the ground is 2.5×10^{-11} radian, and therefore some 2.5×10^6 photons/sec can be collected per pixel (corresponding to a 1 m^2 spot on the ground) at the satellite. With a 10% quantum efficiency of the satellite detector, about 2.5×10^5 photons per second would be detected. This is enough to be useful and to leave a comfortable margin to accommodate a much smaller signal. Of course, much larger signals could be available if the collecting optics were closer to the source of fluorescence.

Not much work seems to have been done to make use of the Fraunhofer lines for remote sensing, and we think that some preliminary scoping studies might be a good investment for DARPA. It is known that many of the Fraunhofer lines are partially "filled in" because of various fluorescing materials on the earth and because of Raman scattering of the sunlight by atmospheric molecules. Systematic investigations of the natural ways that Fraunhofer lines are filled in would be a good start for a DARPA program.

Making a filter to preferentially detect the Fraunhofer wavelengths would be the biggest technical challenge. By separately measuring the intensity of radiation within the Fraunhofer lines of different wavelengths, it would be possible to obtain an approximate spectrum of the fluorescence and thereby characterize the source of the fluorescence. One would need comb filters with linewidths comparable to the equivalent widths of the stronger Fraunhofer lines. DARPA has a program in Fourier optics that could contribute to the development of such filters.

2.5.2 Comb filters

The detailed visible, infrared or ultraviolet spectral properties of materials could be quite useful in characterizing the function of underground facilities. One might hope for spectroscopic identification of the solvents

and organic compounds involved in the production of chemical and biological agents — for example — the characteristic absorption and fluorescent emission spectrum of the amino acid tryptophan. The processing of nuclear materials might also have clear spectroscopic signatures, for example, the characteristic visible spectrum of uranium oxide "yellow cake" or the organic solvents involved in the extraction of Pu and U from irradiated fuel rods. The emission and absorption spectra of the most interesting molecules are very complex in almost every spectral region, from radio frequencies to the ultraviolet. From one point of view, this is bad news since the signal associated with emission or absorption is spread out in a very complicated way over much of the spectrum. There is relatively little information at any given frequency. However, this very complexity can be useful, since the molecule can be viewed as a spread-spectrum transmitter (or absorber) which is amenable to huge processing gains. For convenience, we shall refer to an instrument which can collect and correlate a complicated array of spectral lines as a "comb filter", Comb filters would be of great use for exploiting the Fraunhofer lines of the sun to look for various fluorescent substances. Further discussion of comb filters can be found in the JASON Report "Infrared Comb Filters for Eliminating Background Clutter from Infrared Imaging Systems", by C. Callan and W. Happer (JSR-84-102, JSI 85 053).

There is a limited demand for instruments with comb filters to monitor environmental pollutants like oxides of nitrogen and sulfur, but the market has never been big enough to warrant big investments in technological innovation. Consequently, available comb filters have not benefitted much from modern developments in spread-spectrum signal processing with the most capable modern spectroscopic instruments, for example, those like Fourier transform spectrometers, which are able to utilize all incident photons at once. Very capable comb filters could be constructed with the aid of Fourier-optics components, blazed at multiple frequencies.

Because previous investments in this area have been so limited, and prospects for payoff seem reasonable, some support of innovative work on comb filters would be an appropriate part of a DARPA technology program on UGFs.

2.6 Magnetic Detection of Machinery

On the passive side, there is the idea of searching for static anomalies in the geomagnetic field, such as would be produced by magnetic materials associated with the facility. For terrestrial applications this approach is especially unpromising, owing to the natural background of geological fluctuations. But there is also a passive VLF approach to detection of underground facilities that are in an operating mode. The operations of any facility of interest are likely to rely heavily on electrical machinery. Unless care has been taken to shield the equipment and the structure as a whole, the facility will act as a source of low frequency magnetic disturbances that leak to the outside. The dominant frequencies will be those associated with the rotating electrical machinery as well as that of the power grid (60 Hz or foreign equivalent). At the frequencies in question (we will be imagining frequencies in the interval 10–1000 Hz), the skin depth in soil is large compared to the depth and detection range of any realistic underground facility. The magnetic field outside the facility will therefore fall off with distance as if in free space. We turn now to this passive VLF approach, summarizing and extending the analysis presented in the JASON report JSR-93-140.

The central unknowns have to do with the strength and multipole character of the magnetic fields that are likely to be encountered in association with underground facilities of interest. The dipole component falls with distance as r^{-3}, the quadrupole as r^{-4}, etc. For realistic detection scenarios, we might well be interested in the field strength at distances as large as 1 kilometer. If the dipole component competes at all seriously with the higher

multipoles, it should dominate at such large distances. For orientation: a magnetic dipole of strength 1 amp-m^2 produces a magnetic field $B = 10^{-7}\gamma$ ($1\ \gamma = 10^{-5}$ gauss) at a distance of 1 kilometer. With integration times of order 100 seconds, chosen to overcome instrumental noise, commercially available induction coils should be capable of detecting fields as small as this. For a cartoon, see Figure 2-11.

More limiting than instrumental noise is the background of naturally occurring magnetic fluctuations, produced, for example, by atmospheric lightning (mainly near the equator) and by ionospheric disturbances (occuring mainly near the poles). These perturbations are transported along the ionospheric waveguide channel. The background noise shown as a function of frequency in Figure 2-12 is presumably representative for mid-latitudes. Apart from power line spikes, the noise is seen to fall off with increasing frequency from 1 to several kHz. The dip at that frequency may correspond to a low frequency cutoff below which the waveguide can transport only TE / TEM waves. An over-idealized analysis based on a 2-dimensional waveguide model gives a cutoff frequency of (very roughly) this order. On this interpretation, for the frequency range of interest the background noise arising from the above regions corresponds to disturbances in which the magnetic field is horizontal to the earth's surface (and pointing generally in an east-west direction if the source is in the polar region). It may be, then, that the background can be reduced by measuring the component of B in the vertical direction. Furthermore, although we are not aware of any data bearing on circular polarization, it is possible that background strophic mechanisms cannot easily produce and transport circularly polarized magnetic noise. On the other hand, disturbances produced by electrical machinery will likely be circularly polarized to a substantial degree, different machines (depending on orientation) of course generating different planes (and directions) of circular polarization. This suggests an independent focus on circular polarization, with axis in the horizontal plane.

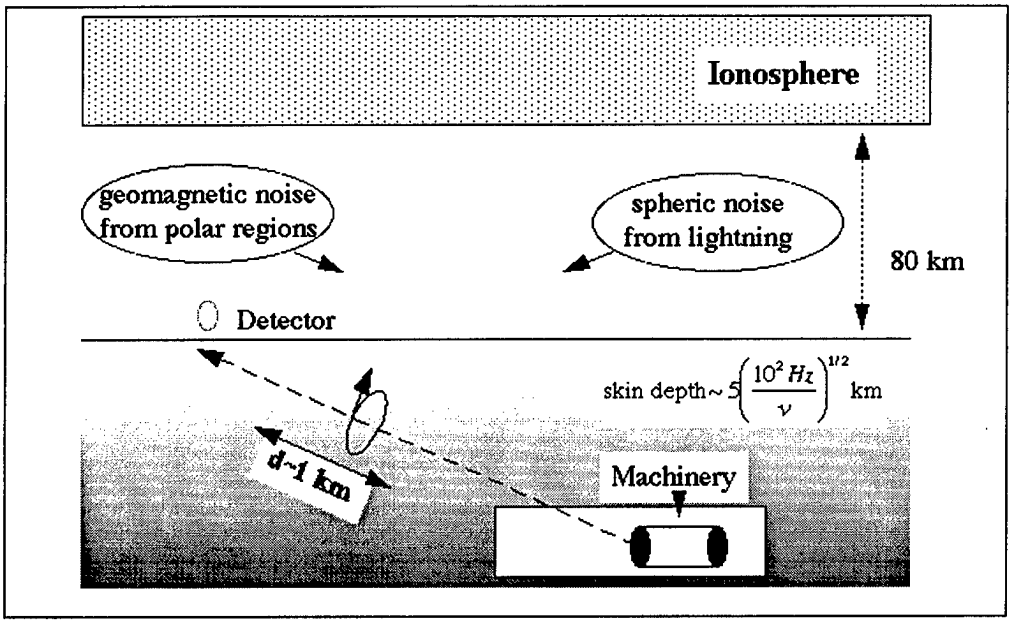

Figure 2-11:

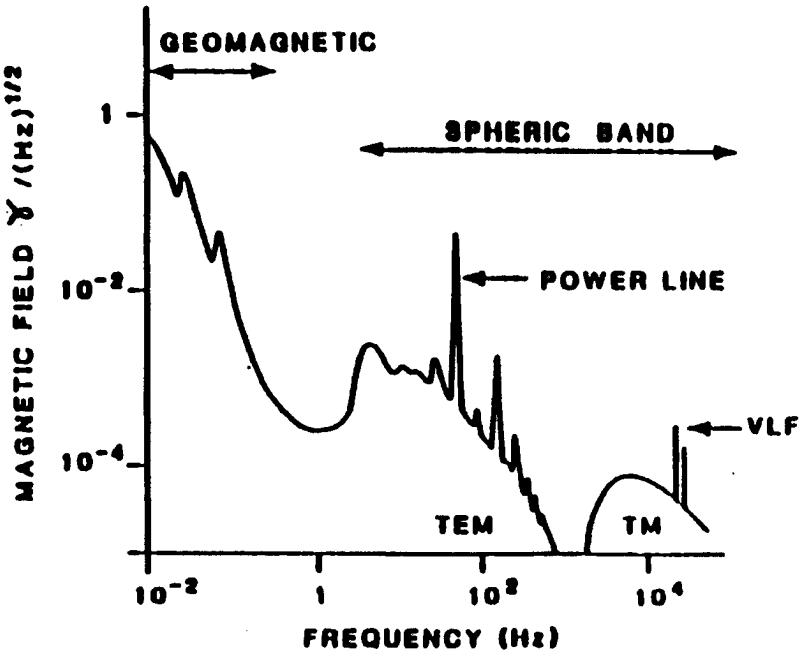

Figure 2-12:

If the idea of passive magnetic detection is to be pursued, one of the earliest tasks will be to form a reasonable estimate of the field strength and multipolarity that might be encountered in association with likely facilities. A good start would be to simply carry out measurements of field strengths around readily available commercial machinery of the kinds likely to be involved. If rough estimates confirm that field strengths at distant detector locations are well above instrument noise, another early task would then be to look more closely at natural magnetic noise as a function of polarization as well as frequency. What we have suggested above is that the noise might be suppressed for the component of B perpendicular to the earth's surface, and suppressed also for circularly polarized components of B with axis in the horizontal plane.

2.7 Other Approaches

2.7.1 Detection of heat shimmer

Casual experience shows that the hot air from vents of buildings can be readily observed at distances of hundreds of meters by the naked eye (and at much greater distance with simple binoculars) because the hot air causes the background scene to shimmer. One might be able to take advantage of this shimmer for remotely detecting the exhaust air of UGFs.

In air of refractive index n, the ideal gas law implies that $n-1$ is inversely proportional to temperature. Gradients of the temperature ΔT will map into gradients of the refractive index of the air. The turbulent, heated air from the vents will cause the background scene to shimmer. The basic limits on detecting shimmer can be understood with the aid of the sketch in Figure 2-13.

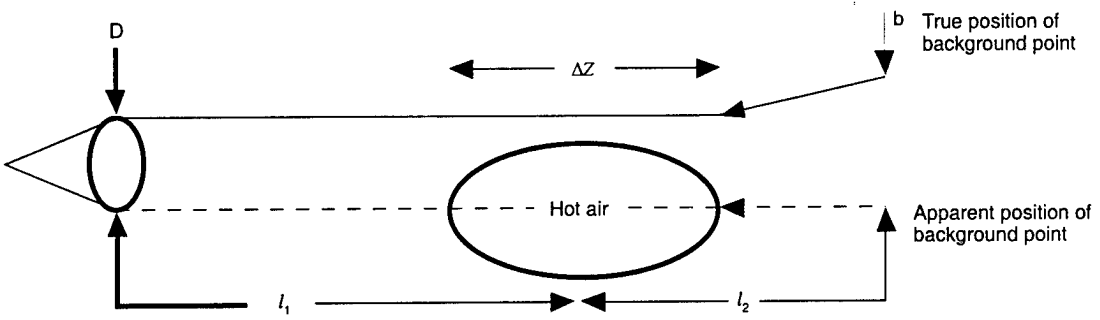

Figure 2-13:

An observer with a lens of diameter D is looking for the deflection of the apparent position of a point in the background scene, located a distance $\ell_1+\ell_2$ away. The apparent position differs from the true position background. The deflection angle θ (in Radians) will be approximately

$$\theta \simeq (n-1)\frac{\Delta T}{T}\frac{\Delta Z}{\Delta X}$$

where ΔZ is the distance of the heated air along the line of sight, and ΔX is the effective distance transverse to the line of sight over which the temperature changes from warm to ambient values at the edge of the plume of exhaust air. For representative values $n-1 = 10^{-3}$, $\Delta Z = 3$ m, $\Delta X = 0.3$ m and $\Delta T = 30$ K, T=300 K the deflection angle will be

$$\theta \simeq 10^{-3}.$$

If the distance from the hot air to the background point is ℓ_2, then the apparent deflection of the background point is $\theta\ell_2$. For an ideal optical observing system with diffraction limited optic, the apparent radius of the background point (the resolution limit) can be no smaller than $(\ell_1+\ell_2)\frac{\lambda}{D}$, so the ratio of the apparent deflection to the resolution limit is

$$r = \frac{\theta D \ell_2}{\lambda(\ell_1+\ell_2)}.$$

The deflections estimated above can be recognized because the apparent position of the background point will fluctuate as the turbulent exhaust gas moves, and it is this shimmering motion that is the signature of the warm exhaust air. Because the relative deflection r is proportional to the distance ℓ_2 from the exhaust gas to the background, the shimmer is most easily seen if it is observed against a distant background. Detection from overhead assets will be very difficult since the "lever arm" ℓ_2 would only be a few meters.

For example, a ground observer viewing the vented air from a suspected UGF located $\ell_1 = 3$ km away against a background features $\ell_1 + \ell_2 = 10$ km away with optics of diameter 6 cm ($D = 6$ cm) with visible light of wavelength $\lambda = 600$ nm would find the readily detectable ratio

$$r = 110.$$

Observation from near the ground rather than from an overhead platform is almost essential because a distant background is needed to make the heat shimmer readily visible. However, the observation point could be several km away from the suspected UGF, and the required optical equipment could be relatively simple.

Neutrino and Muon Tomography

The great penetrating power of neutrinos and high energy muons, the fact that their interaction probabilities with matter are proportional to the total mass traversed, and their ubiquitous presence around the earth have led to suggestions that they be used to detect underground structures. Indeed, Alvarez in the 1960's "x-rayed" the Second Pyramid of Giza with cosmic-ray muons detected in spark chambers placed under it. (He found no unknown structures!) de Rujula, *et al.* (*Physics Reports* **99**, No. 6 (1983) 341-396. North-Holland Pub.) studied possibilities for prospecting on a large scale using high energy neutrinos from TeV-scale accelerators and modern detector techniques. JASON prepared an earlier primer (Neutrino Detection Primer, JSR-84-105, March 1988) on relevant physics issues. While interesting and

important scientifically, this body of work indicated the complete impracticality of using neutrinos or muons as a sensor for underground structures.

More recently, massive ($> 10^4$ ton) underground detectors have made solar neutrino detection "routine" and are beginning to make convincing cases for detection of "upward-going" neutrinos that have penetrated the entire earth. However, there is no new evidence to suggest that neutrinos or muons are, in any way, useful for detecting or characterizing underground structures.

2.7.2 Gravimetry

Two types of gravimetry are considered here, the direct measurement of gravity anomalies and gravity gradiometry. Of these two, anomaly detection has dominated in exploration geophysics, but it appears to be only marginally promising for the problem at hand because the natural and artificial backgrounds are high (including acceleration-induced noise on moving platforms) and the spatial resolution is consequently poor. Very recently, gradiometry has emerged as a potentially useful technology for detecting UGFs.

2.7.2.1 Gravity anomalies

Gravity anomalies, the spatial variation in gravitational acceleration due to subsurface density variations, can be measured from moving platforms with a precision of about 1 mgal (10^{-3} cm/s^2). To gain an appreciation for the rough magnitudes involved, consider an empty cylinder of radius R and infinite length buried at a depth Z in material of density r; this simulates a tunnel of length $\geq R$. The maximum amplitude of the resulting gravity anomaly is

$$\Delta g_Z(\text{mgal}) = 0.2 \left(\frac{R}{5\text{ m}}\right)^2 \left(\frac{(Z+h)}{10\text{ m}}\right)^{-1} \left(\frac{\rho}{2\ g\ \text{cm}^3}\right)$$

where h is the height of the gravimeter above the surface and Δg_z is the

perturbation in the vertical component of gravitational acceleration that is usually measured. Thus, a rather large chamber (10 m diameter) buried just below the surface (5 m depth) would not exceed the detection limit (1 mgal) even from a vehicle flying at very low altitude (10 m) above the surface. Unless significant improvements in sensitivity are possible, the results are not very promising.

Somewhat more promising, but still difficult, are measurements from a vehicle on a road (e.g., a van or car). The documented sensitivity of car-borne measurements is comparable to that for airborne measurements ($\sim$ 1 mgal), although there is some possibility that the detection limit could be improved to as low as $\sim$ 0.1 mgal. If so, near-surface or structures such as basements, or possibly large tunnels at shallow depths, might be detected. However, little additional information would be provided other than the identification of a void at depth.

If made when stationary, the measurements can approach the limit of resolution of modern gravimeters, i.e., $\sim$0.01 mgal. With very careful use, a factor of 10 better resolution might be achievable. Taking the 10 μgal as a fiducial sensitivity, structures at 50 m depth might be detectable. Of course, even crude information about size and shape require multiple measurements from several locations. An added problem at this level of resolution is that stations must typically be reoccupied in order to remove secular drift, both of the instrument and due to natural causes (e.g., tides).

Given the operational difficulty of making very careful measurements from a stationary sensor at multiple locations, and the limited information that is provided, we do not view the detection of gravity anomalies as a promising approach for UGF characterization unless there is a significant improvement in the technology.

2.7.2.2 Gravity gradients

Gravity gradiometry presents some advantages to the direct measurement of anomalies, especially from moving platforms. Using current technology, it is possible to essentially null out the instrument drift and acceleration-induced noise from the platform. Although more challenging to measure in some respects, gravity gradients have the advantage of enhanced spatial resolution in comparison with the anomalies themselves. This method has advanced significantly with the recent declassification of technology that was initially developed for submarine navigation.

Considering again the infinite cylinder as a model for a tunnel of radius R at depth Z in a medium of density ρ, the maximum vertical gradient occurs right over the axis of the cylinder and is of magnitude

$$\partial \Delta g_Z / \partial Z(\mathrm{E}) = 838 \left(\frac{\mathrm{R}}{(\mathrm{Z} + \mathrm{h})} \right)^2 \left(\frac{\rho}{2 \text{ g cm}^3} \right)$$

if measured from a height h. The dimensions are in Eötvös (= 0.1 μgal/m or 10^{-9} s^{-2}), and detection limits of about 0.5-1.0 E have been obtained from relatively small (< 1 m maximum dimension) ship-borne and airborne instruments. This means that a measurable signal, exceeding 1 E, can be found for a tunnel in a $\rho = 2$ g/cm^3 medium as long as $Z + h \leq 29\ R$: a 5 m radius tunnel at a depth of 45 m can be observed from a height of 100 m.

Development is in progress of instruments theoretically capable of 0.1 E resolution. However, it is not clear that these will be small enough to be of practical use for UGF detection or characterization. More promising would seem to be the prospect of fielding an array of gradiometers because, even with the current sensitivity, the added redundancy and the spatial pattern that is collected should be possible to identify anomalous features (e.g., a linear void) at even greater depths than suggested by the above estimate. Thus, gradiometry obtained from UAVs could provide a powerful means of identifying the presence, shape and dimensions of a UGF.

2.8 Lessons Learned from Tunnel Hunting in Korea

Extensive efforts to find tunnels running from north to south under the demilitarized zone (DMZ) in Korea have been going on for some 23 years, 1974 to date. During the period 1974 to 1990 four tunnels were discovered in 16 years (*New York Times*, 1988 and 1990). This effort involved hundreds of personnel in the Republic of Korea and U. S. Armies, headed by the United Nations Tunnel Negation Team. This clearly shows that finding tunnels is a very difficult problem. The tunnel locations are shown in Figure 2-14.

Figure 2-14: Tunnels across the DMZ in Korea, discovered 1974–1990.

The tunnels in the west were presumably built to support an attack across the DMZ toward Seoul. Tunnels in the eastern mountains are particularly hard to find and confirm because of the difficult terrain. At least one drill rig has been lost in these mountains.

The persistent efforts to find tunnels under the DMZ involved the following:

1. Careful handling of defectors to discover very precise information on tunnel locations.
2. Extensive intelligence data analysis, including aerial photography along the DMZ.
3. Extensive drilling, often to depths of hundreds of feet, by a fleet of drilling rigs.
4. Seismic listening, cross borehole electromagnetic sounding, down borehole. sensors (magnetometers, etc.) and other geophysical exploration techniques.

Given this information the tunnels that were discovered were found mainly due to defector information and North Korean mistakes as well as a number of lucky breaks. The drilling and geophysical exploration methods were mainly used for localization, often on the basis of defector information.

Although a number of tunnels have been found, defector information indicates that about a dozen tunnels were completed as of the 1970's. The number of incidents involving North Korean infiltrators in these and later years may indicate that there were, and perhaps still are, a number of tunnels in use as infiltration routes.

Some lessons learned from the Korean experience, and from Vietnam as well [10], are as follows:

1. Even with access on the ground, as well as aerial surveillance, and extensive efforts over many years, underground structures are very hard to find, especially if deep (> 30 m).

2. A determined foe can disguise construction effectively in many locations. For example, the North Koreans disguised drill and blast tunnel construction by covering the seismic signals due to blasting with nearby artillery practice.

3. Success depends on the persistent use of a wide spectrum of information over a significant time span. In Korea this information includes defector and other types of intelligence information, seismic listening, electromagnetic sounding, drilling and borehole sensors [13].

4. In Korea the most important source of information was via defectors. As conditions in North Korea have become worse, there has been an increase in defectors and perhaps some new tunnels will be discovered as a result.

3 COVERT vs. OVERT FACILITY CHARACTERIZATION

3.1 Comparison of Methods

As discussed elsewhere in this report, our emphasis is not on detection of underground facilities, but on characterizing them. Without detailed plans and humint it is difficult to imagine knowing much more about a denied facility than a general picture of its size and shape and its function (e.g., chemical warfare factory, nuclear weapons storage). We will therefore begin by comparing the methods briefed to us, plus a couple of JASON inventions, with respect to their ability to discover size, shape, and function, as well as their potential standoff distance from the site and their possibility for covertness. As to size and shape we use a single figure of merit, which is the claimed spatial resolution of the technique.

It will turn out that most if not all techniques are really quite short-range, and thus are not likely to be useful for characterization in countries where overt overflights and other forms of overt visitation are denied or restricted. The question of whether a technique can be used covertly then becomes important. We do not discuss direct placement and recovery of sensors in the facility by humans, which is an issue for the intelligence community, although it would certainly be helpful (for example, a covert GPS/inertial navigation system device mounted on a tunnel-boring machine would give far more detailed information about size and shape than anything we discuss here). For us a covert device will be one that can be placed outside but close to the facility, possibly by air drop, which is hidden from casual visual inspection, and which needs no visits by humans—in short, an unattended ground sensor (UGS). Numerous variations can be considered; for example,

in a previous JASON report [14] we observed that it may be possible to place a passive acoustic or seismic array of geophones covertly by airdrop, and in time of urgent necessity an active source (small bombs) could be used on a time scale too short to be countered by the occupants of the underground facility, but of course giving away the show.

Table 3.1 below gives the comparison of methods mentioned above and is a copy of Table 1.1.

Table 3.1

Method	Characterization Ability	Standoff?	Covert?	Outlook
Imagery/ Change Detection	Adits, Shape	Aircraft/Satellite	Yes	Promising
Power Lines	Machinery current/voltage	~100 m	Yes	Promising
Spectroscopy (Fraunhofer, etc.)	Effluents; Nuclear	Aircraft/Satellite	Yes	Promising
Vibration Sensing	Presence/Location of machine	Laser: Aircraft/Satellite Geophone: $\leq$ 1 km	Yes	Promising
Chem/Bio Sensors	Chem/bio signatures	No	Maybe	Promising
Passive EM	Location of machinery	~ km	Yes	Uncertain
Passive Seismic Imaging	Size, Shape	~100 m	Yes	Uncertain
Active Seismic Imaging	Size, Shape	~100 m	No	Uncertain
EM Induction	Size, Shape	No	Maybe	Not promising
Gravity Gradiometer	Size, Shape	~100 m	Maybe	Uncertain

3.2 Discussion of Covertness Possibilities

There has been a great deal of work on UGSs, including their use for counterproliferation; for example, reference [7]. We need not repeat that analysis here. It discusses primarily techniques for vapor and liquid analysis, including power requirements, available batteries, deployment by micro-UAVs, and other means.

The requirements for covert deployment and covert function of an UGS are that it be sufficiently small to be deployed from a remote platform and to be concealed; that it have sufficient power to function for a long time; and that transmission of its data be covert. The problems are quite different

in urban areas and in remote areas far from cities, and we will not discuss the urban problem here; it is likely to be involved with placements involving human association with the sensor.

In remote areas the likely method of deployment is by airdrop. Note that the necessary overflight itself may be detected; what is important is to conceal the deployment, which therefore will likely take place at night. Most of the sensors in Table 3.1 can be made rugged enough to survive an airdrop with no parachute, and such a deployment may even be preferable. An example is an acoustic or seismic array consisting of geophones (and ancillary equipment) on a spike which needs to penetrate the ground for good acoustic coupling. But making a laser vibrometer rugged enough to survive an unbraked landing from an aircraft is problematic.

For some UGSs, either delivery to a precise location or precise knowledge of the location, even though delivery is not well-controlled, is essential. An effluent sensor will do better the closer it is to an airshaft or other facility vent, for example. Or one may conceive of an inductive tap closed around a power line high above the ground, which can measure the impedance and phase variations on the line, and which must be placed directly around the line. Here precise delivery is absolutely essential. It might be accomplished with a micro-UAV launched from a larger aircraft at some distance away. Again, the micro-UAV itself may be discovered later, but the hope would be that it can deliver the sensor undetected.

An acoustic array of geophones need not be deployed with tremendous accuracy, but the locations of the geophones must be known to within perhaps half a wavelength or better. This could be done with GPS receivers, but these receivers use a fair amount of power, and may yield marginal location accuracy. Another location method employs corner cubes (concealed, for example, in a fake rock) and a SAR to find the locations. It is also possible to use the corner cube to transmit data more or less covertly and with essentially no power to the SAR receiver. The trick is to have one or more faces of the

corner cube made of antenna elements covering the SAR bandwidth, with the antenna elements interrupted at strategic locations on the corner-cube face with FET switches. When the switches are in one position the antenna functions as a normal reflecting face; in another position, antenna function is disrupted, either by breaking continuity or by inserting appropriate reactive impedances. This is a well-known technique for changing radar cross-section [15]. Modulation of the corner cube at the SAR slow-time rate should allow transmission of data at a rate of tens to hundreds of bits per second. This SAR technique for geolocation and for passive data transmission is discussed in more detail in another of this summer's JASON reports [16].

4 ASSESSMENT OF POSSIBLE AREAS FOR FUTURE R&D

We summarize our findings by recommending possible areas for DARPA R&D investment. As described in the introduction to this report, we have emphasized technologies which could payoff when applied to the problem of characterization of UGFs, with particular attention to those methods that might be used in a standoff or covert mode.

Ground Sensors

We recommend development of a suite of small ground sensors with remote interrogation or communication capability via laser or RF link. Examples include:

- Low-power compact geophones
- Low-power EM field detectors
- Miniaturized imagers
- Chemical and biological sensors.

Supporting generic technologies include:

- Covert communications
- Power systems
- Covert precision placement
- MEMS.

Vibration Sensing

In our opinion, vibration sensing has significant potential for providing valuable information on UGFs, particularly if it is employed during the construction phase of the UGF when localization of tunnel boring machines can yield information on the tunnel geometry.

We strongly recommend further R&D in the following areas:

- Use of arrays of sensors to localize and, possibly characterize signal sources such as tunnel borers, pumps, generators, and fans;
- Use of laser vibrometry for standoff methods. Research should include use of differential techniques to mitigate atmospheric effects and opportunistic use of surface features ("acoustic antennas") such as ducts, flagpoles, trees, etc.

Specific objectives should include:

- Demonstration of localization capability to accuracies better than 10 meters using arrays of standard geophones;
- Development of a low-power covert sensor consisting of a geophone or equivalent MEMS sensor and a covert com link;
- Detection of a subsurface tunnel boring machine using a conventional Doppler laser on an airborne platform;
- Development of covert differential retroreflectors.

Power Lines

We recommend further study of ways to use power lines to characterize UGFs. Areas of study include ways to:

- Map feeder networks (also useful for detection of UGFs),
- Monitor currents (standoff and in-situ methods),
- Insert and extract characteristic signals.

Imagery and Change Detection

Significant opportunities exist for exploiting imagery information, particularly if change detection methods can be employed. We make the following recommendations:

- Collect baseline information (visible, infrared, SAR) as early as possible in areas where UGF activity is suspected for exploitation in change detection analysis.
- Apply processing techniques that emphasize detection of UGF features. In particular, we have noted that standard SAR processing techniques are not optimal for UGF signatures (e.g. adits and vents) and we have suggested alternative algorithms.
- Development of an interferometric SAR system for a UAV platform. Interferometric SAR data collected over known UGFs would be very useful in detection of openings such as ducts and vents.

Multispectral Imaging

There may be unrealized potential for multispectral observations of the characteristic emission and absorption spectra of effluents from nuclear, chemical, and biological weapons production. Specific areas for further study include:

- Measurements of the level of background "clutter" for multispectral measurements in natural environments.

- Investigation of the use of the dark Fraunhofer absorption lines in the solar spectrum to allow daytime detection of the fluorescence signature of effluents.

- Development of selective filters for Fraunhofer line, e.g. using holographic techniques.

Low-Frequency EM

We recommend that controlled experiments for magnetic signals from machinery be carried out, together with measurements of the magnetic noise spectrum at various geographic locations. Specifically we recommend:

- Compilation of a catalog of characteristic frequency spectra from pumps, centrifuges, generators, etc., both for continuous operation and start-up transients.

- Measurement of the circular polarization characteristics of spheric and geomagnetic noise.

- Investigation of adaptive nulling of noise by use of multiple sensors at widely-spaced locations.

- Assessment of the possibility of introducing magnetic signatures into critical machinery (e.g. small magnetized regions on pumps or centrifuges).

We are less impressed with attempts to use low-frequency ionospheric waves to image UGFs. DARPA should continue to monitor such programs for feasibility, both from a physics standpoint and from the standpoint of operational complexity.

A APPENDIX: SAR Simulation Program

```
/* main.c */
/* ---------------------------------------------------------- */
define ADIT 0.0 /* Assummed Depth of the ADIT for processing */
define HEIGHT 20.0 /* Height of the observation platform */
define NPULSES 121 /* Number of RADAR pulses along the track */
define NBINS 94 /* Number of range bins in RADAR */
define NTARGET 2 /* Number of targets */
define PLOTSZ 60 /* Size of SAR plot */
define PLOTGN 0.0065 /* Gain for SAR plot */
/* ---------------------------------------------------------- */
include¡stdio.h¿
include¡stdlib.h¿
include¡math.h¿

FILE *fp;

float x[] =  10.0, 10.0, 18.90, 22.6 ; /* Targets at (x,y) with RADAR cross */
float y[] =  30.0, 30.0, 30.00, 30.0 ; /* section s and adit depth z */
float s[] =  1.0, 1.0, 0.00, 0.0 ;
float z[] =  0.0, 5.1, 0.00, 0.0 ; /* ADIT depth set at 5.1 */

void sarplot(void);
float gamm(long, long);
float phi(long);
void plotsig();
float sig(float, float);
float pulse( float, float);

float a, h2;

void main(void)

h2 = HEIGHT*HEIGHT;
a = h2 + x[0]*x[0] + y[0]*y[0];
sarplot(); return;
plotsig();
return;
/* End of main program */

/* ---------------------------------------------------------- */
void sarplot(void)

long i,j,k;
float r;

if(ADIT¿0.0) printf(" Adit Image Processing: ");
else printf(" Ground Inage Processing: ");
```

```
printf(" Plot gain = printf(" Target cross section = printf(" Adit cross section =
for(i = 0;i¡PLOTSZ; i++)  printf("-"); ;
for(i = 0; i¡PLOTSZ/2; i++)

printf("—");
for(j=0;j¡PLOTSZ;j++)

r = PLOTGN*a*gamm(i,j);
r = r*r;
k = 2.0*r;
if(r¿0.3) printf( ";
;
printf("—");
for(i = 0; i¡(PLOTSZ/2)-3; i++)  printf("-"); ;
printf("END");
for(i = PLOTSZ/2;i¡PLOTSZ; i++)  printf("-"); ;



float gamm(long x, long y)

float d, d2, g;
long ti, cy;
g = 0.0;
for(cy = 0; cy ¡ NPULSES; cy++)

for(ti= 0; ti¡ NBINS; ti++)

d2 = h2 + x*x + (y-cy)*(y-cy);
d = sqrt(d2) + ADIT;
g = g + sig(ti, cy)*phi(ti - 2.0*d);
;
;
return(g);


float phi(long k)  if(k==0) return(3.29); return(-1.0/(k*k));  /* Discrete Mexican Hat
function */

void plotsig(void )

long k, cy, ti;
float u,v,r;
/* printf("————————————————————————————START————————————————————————————-");
*/
for(cy = 0; cy ¡ NPULSES; cy++)

printf("—");
for(ti= 0; ti¡ NBINS; ti++)

r = a*sig(ti, cy);
```

```
k = 2.0*r;
if(r¿0.05) printf( ";

printf("————————————————————————END————————————————————————");

float sig(float ti, float cy)
float r, d, d2;
long j;
for(j =0, r= 0.0; j¡NTARGET;j++)

d2 = h2 + x[j]*x[j] + (y[j] - cy)*(y[j] - cy) ;
d = sqrt(d2) + z[j];
r = r + (1.0/d2)*s[j]*pulse(d,ti);
;
return(r);


float pulse( float d, float ti)

float t,t0,t1,t2;
t = 2.0*d; /* t = 2.0*d/C ; */
t0 = t - ti;
t1 = t0 + 1;
t2 = 2.0 - t1;


      if((t1¿0)(t2¿0)) if(t0¡0) return(t1); return(t2);;

return(0.0);


/* ————————————————————————————————————————————
/
```

References

[1] "Baselining of Sensor Technology for Detecting and Characterizing Underground Facilities", Dec. 1995.

[2] Berger, R., et al., "Characterizing an Underground Chemical Weapons Production Facility - Summary Report", July, 1996.

[3] Berni, A. J., "Remote Sensing of Seismic Vibrations by Laser Doppler Interferometery", *Geophysics*, **59**, 1856-1867 (1994).

[4] Kirby, A., W. Philipson, R. Gee, and C. Searls, "Underground Facility Detection and Characterization",

[5] "1996 Annual Report of the Underground Activities Focus Group", Feb. 1997.

[6] Lewis, N., et.al., "Technologies for Monitoring Proliferation of Weapons of Mass Destruction: Detection of Underground Facilities", JASON Report JSR-93-140 (1995).

[7] Lewis, N., et al., "Unattended Ground Sensor for Counterproliferation Applications", JASON Report JSR-94-140A (1997).

[8] Attewell, P. B., J. Yeates and A. R. Selby, *Soil Movements Induced by Tunnelling and their Effects on Pipelines and Structures*, Blackie, Glasgow and London (1986).

[9] Massonnet, et al., "The Displacement Field of the Landers Earthquake Mapped by Radar Interferometry", *Nature* **364**, 138-142 (8 July, 1993).

[10] Mangold, T. and J. Penycate, *The Tunnels of Cu Chi*, Berkley Books, NY (1985).

[11] New York Times, "Seoul Uncovers a Border Tunnel", *New York Times* (March 4, 1990).

[12] New York Times, "S. Korea's Security Tourism Offers Tunnel View", *New York Times* (July 25, 1988).

[13] Vesecky, J. F., W. A. Nierenberg, and A. M. Despain, "Tunnel Detection", JASON Tech. Rpt. JSR-79-11, SRI International, Arlington, VA (1980).

[14] Cornwall, JM., et al., "Precision Strike", JASON Report JSR-92-171 (1992).

[15] Ruck, G. T., et al., *Radar Cross-Section Handbook*, Vol. 2 (Plenum, New York, 1970).

[16] Fortson, N., et al., "Small Unit Operations", JASON Report JSR-97-140 (1997).

DISTRIBUTION LIST

Director of Space and SDI Programs
SAF/AQSC
1060 Air Force Pentagon
Washington, DC 20330-1060

CMDR & Program Executive Officer
U S Army/CSSD-ZA
Strategic Defense Command
PO Box 15280
Arlington, VA 22215-0150

Superintendent
Code 1424
Attn Documents Librarian
Naval Postgraduate School
Monterey, CA93943

DTIC [2]
8725 John Jay Kingman Road
Suite 0944
Fort Belvoir,VA 22060-6218

Dr. A. Michael Andrews
Director of Technology
SARD-TT
Room 3E480
Research Development Acquisition
103 Army Pentagon
Washington, DC 20301-0103

Dr. Albert Brandenstein
Chief Scientist
Office of Nat'l Drug Control Policy
Executive Office of the President
Washington, DC 20500

Dr. H. Lee Buchanan, III
Assistant Secretary of the Navy
(Research, Development & Acquisition)
3701 North Fairfax Drive
1000 Navy Pentagon
Washington, DC 20350-1000

Dr. Collier
Chief Scientist
U S Army Strategic Defense Command
PO Box 15280
Arlington, VA 22215-0280

D A R P A Library
3701 North Fairfax Drive
Arlington, VA 22209-2308

Dr. Victor Demarines, Jr.
President and Chief Exec Officer
The MITRE Corporation
A210
202 Burlington Road
Bedford,MA01730-1420

Mr. Frank Fernandez
Director
DARPA/DIRO
3701 North Fairfax Drive
Arlington, VA 22203-1714

Mr. Dan Flynn [5]
Deputy Chief
OSWR
CDT/OWTP
4P07, NHB
Washington, DC 20505

Dr. Paris Genalis
Deputy Director
OUSD(A&T)/S&TS/NW
The Pentagon, Room 3D1048
Washington, DC 20301

Dr. Lawrence K. Gershwin
NIO/S&T
2E42, OHB
Washington, DC 20505

Mr. David Havlik
Manager
Weapons Program Coordination Office
MS 9006
Sandia National Laboratories
PO Box 969
Livermore, CA94551-0969

Dr. Helmut Hellwig
Deputy Asst Secretary
(Science, Technology and Engineering)
SAF/AQR
1060 Air Force Pentagon
Washington, DC 20330-1060

Dr. Robert G. Henderson
Director
JASON Program Office
The MITRE Corporation
1820 Dolley Madison Blvd
Mailstop W553
McLean, VA 22102

DISTRIBUTION LIST

J A S O N Library [5]
The MITRE Corporation
Mail Stop W002
1820 Dolley Madison Blvd
McLean, VA 22102

Mr. O' Dean P. Judd
Los Alamos National Laboratory
Mailstop F650
Los Alamos, NM 87545

Dr. Bobby R. Junker
Office of Naval Research
Code 111
800 North Quincy Street
Arlington, VA 22217

Dr. Martha Krebs
Director
Energy Research, ER-1, Rm 7B-058
1000 Independence Ave, SW
Washington, DC 20858

Lt Gen, Howard W. Leaf, (Retired)
Director, Test and Evaluation
HQ USAF/TE
1650 Air Force Pentagon
Washington, DC 20330-1650

Dr. John Lyons
Director of Corporate Laboratory
US Army Laboratory Command
2800 Powder Mill Road
Adelphi,MD 20783-1145

Dr. Arthur Manfredi
ZETA Associates
10300 Eaton Drive
Suite 500
FairfaxVA 22030-2239

Dr. George Mayer
Scientific Director
Army Research Office
4015 Wilson Blvd
Tower 3, Suite 216
Arlington, VA 22203-2529

Ms. M. Jill Mc Master
Editor
Journal of Intelligence Communication
Investment Program Office (IPO)
1041 Electric Avenue
Vienna,VA 20180

Dr. Thomas Meyer
DARPA/DIRO
3701 N. Fairfax Drive
Arlington, VA 22203

Dr. Bill Murphy
ORD
Washington, DC 20505

Dr. Julian C. Nall
Institute for Defense Analyses
1801 North Beauregard Street
Alexandria, VA 22311

Dr. Ari Patrinos [5]
Associate Director
Biological and Environmental Research SC-70
US Department of Energy
19901 Germantown Road
Germantown,MD 207874-1290

Dr. Bruce Pierce
USD(A)D S
The Pentagon, Room 3D136
Washington, DC 20301-3090

Mr. John Rausch [2]
Division Head 06 Department
NAVOPINTCEN
4301 Suitland Road
Washington, DC 20390

Records Resource
The MITRE Corporation
Mailstop W115
1820 Dolley Madison Blvd
McLean,VA 22102

Dr. Victor H Reis [5]
US Department of Energy
DP-2, Room 4A019
Mailstop 4A-028
1000 Independence Ave, SW
Washington, DC 20585

Dr. Fred E. Saalfeld
Director
Office of Naval Research
800 North Quincy Street
Arlington, VA 22217-5000

DISTRIBUTION LIST

Dr. Dan Schuresko
O/DDS&T
OSA/ATG
Room 23F20N, WF-2
Washington, DC 20505

Dr. John Schuster
Submarine Warfare Division
Submarine, Security & Tech
Head (N875)
2000 Navy Pentagon Room 4D534
Washington, DC 20350-2000

Dr. Michael A. Stroscio
US Army Research Office
P. O. Box 12211
Research Triangle Park,NC27709-2211

Ambassador James Sweeney
Chief Science Advisor
USACDA
320 21st Street NW
Washington, DC 20451

Dr. George W. Ullrich [3]
Deputy Director
Defense Special Weapons Agency
6801 Telegraph Road
Alexandria, VA 22310

Dr. David Whelan
Director
DARPA/TTO
3701 North Fairfax Drive
Arlington, VA 22203-1714

Dr. Edward C. Whitman
US Naval Observatory
Nval Oceanographers Office
3450 Massachusetts Ave, NW
Washington, DC 20392-5421